

**Sensing *Botrytis cinerea* in Tomato Using Visible/Near-Infrared
(VIS/NIR) Spectroscopy**

By:

Khadija Mohammad Khames Najjar

Supervisor:

Dr. Nawaf Abu-Khalaf

This Thesis was Submitted in Partial Fulfillment of the Requirements

for the Master Degree of Science in:

Agricultural Biotechnology

Deanship of Graduate Studies

Palestine Technical University-Kadoorie (PTUK)



June, 2020

استشعار وجود الفطر المسبب للعفن الرمادي في البندورة باستخدام الاشعة المرئية

والقريبة من تحت الحمراء

الطالبة:

خديجة محمد خميس نجار

المشرف:

الدكتور نواف أبو خلف

قدمت هذه الرسالة استكمالاً لمتطلبات الحصول على درجة الماجستير في:

التكنولوجيا الحيوية الزراعية

عمادة الدراسات العليا

جامعة فلسطين التقنية-خضوري



حزيران، 2020

Committee Decision

This thesis/dissertation (Sensing *Botrytis cinerea* in Tomato Using Visible/Near-Infrared (VIS/NIR) Spectroscopy) was successfully defended and approved on 10/Jun/2020.

Examination committee

Signature

-Dr. Nawaf Abu-Khalaf, (supervisor) _____

Assoc. Prof. / College of Agricultural Sciences and Technology,
Palestine Technical University-Kadoorie (PTUK).

- Prof. Hassan Abu-Qaoud, (External Examiner) _____

Prof. / College of Agriculture and Veterinary Medicine,
An-Najah National University.

-Dr. Daoud Abu-Safieh, (Internal Examiner) _____

Assistant Prof. / College of Agricultural Sciences and Technology,
Palestine Technical University-Kadoorie (PTUK).

جامعة فلسطين التقنية-خضوري

نموذج التفويض

انا الطالبة خديجة محمد خميس نجار، أفوض جامعة فلسطين التقنية-خضوري بتزويد نسخ من رسالتي/أطروحتي للمكتبات والمؤسسات أو الهيئات أو الاشخاص عند طلبهم حسب التعليمات النافذة في الجامعة.

التوقيع:

التاريخ: 10/Jun/2020

Palestine Technical University-Kadoorie

(PTUK)

Authorization form

I, Khadija Mohammad Khames Najjar, authorize the PTUK to supply copies of my thesis/ dissertation to libraries or establishments or individuals on request, according to the university of PTUK regulations.

Signature: _____

Date: 10/Jun/2020

**Sensing *Botrytis cinerea* in Tomato Using Visible/Near-Infrared
(VIS/NIR) Spectroscopy**

By:

Khadija Mohammad Khames Najjar

Supervised by:

Dr. Nawaf Abu-Khalaf

قدمت هذه الرسالة استكمالاً للمتطلبات الحصول على درجة الماجستير في:

التقانة الحيوية الزراعية

This Thesis was Submitted in Partial Fulfillment of the Requirements

for Master Degree in:

Agricultural Biotechnology.

Deanship of Graduate Studies

عمادة الدراسات العليا

Palestine Technical University-Kadoorie

جامعة فلسطين التقنية-خضوري

June/ 2020

حزيران/2020

**Sensing *Botrytis cinerea* in Tomato Using
Visible/Near-Infrared (VIS/NIR) Spectroscopy**

Dedication

This thesis is dedicated to the source of support for me, my dear parents. Also, to my brothers and sister, those who supported me during my studies in general and during the preparation of this research in particular.

Moreover, dedicated to my friends, who are the source of my confidence and strength.

Finally, it is dedicated to everyone who provided me assistance, support, and guidance or advice from the beginning of the study until the last moment in its preparation.

Acknowledgement

First of all, I thank Allah so much for inspiring me to write this thesis. Also, I would like to thank my family for supporting me. I also thank my academic supervisor Dr. Nawaf Abu-Khalaf for his guidance and for helping me to prepare this thesis in the way it is now. Thanks also to my friends: Ruya Abu-Alfaya, Basima Abu-Rumiala and Amal Abu-Diab for helping me during the study period.

Finally, I would like to thank Palestine Technical University-Kadoorie (PTUK) for offering me a scholarship for excellent efforts during my Master's studies, as well as financial support for this research.

Table of contents

Committee Decision	III
Dedication	VII
Acknowledgement	VIII
Table of contents	IX
List of Tables	XII
List of Figures	XIII
List of Abbreviations/Symbols	XVII
Abstract	1
1 Introduction	3
1.1 General introduction.....	3
1.2 Aim.....	5
1.3 Objectives.....	5
2 Literature Review	6
2.1 Tomato crop importance and production	6
2.2 Food safety and quality	7
2.3 Gray mold.....	8
2.4 Methods for plant disease detection	10
2.4.1 Using a PCR to identify plant disease pathogens	11
2.4.2 Non-destructive methods for plant disease detecting	12
2.4.2.1 Visible/near-infrared spectroscopy	12
2.4.2.2 Visible/near-infrared spectroscopy applications	17

2.4.2.3	Visible/near-infrared technology advantages and limitations	18
2.4.2.4	Visible/near-infrared spectral data analysis.....	19
2.4.2.4.1	Multivariate data analysis (MVDA).....	19
2.4.2.4.2	Principal component analysis (PCA).....	20
2.4.2.4.3	Pre-processing of spectral data.....	22
2.5	Visible/near-infrared spectroscopy application for plant diseases detection	23
3	Materials and Methods.....	25
3.1	Fungal methods	25
3.1.1	Media preparation	25
3.1.2	Isolation and identification of the fungi.....	25
3.1.3	Morphological identification	27
3.1.4	Molecular identification.....	27
3.1.4.1	Fungal DNA extraction	27
3.1.4.2	Polymerase chain reaction (PCR).....	28
3.1.4.2.1	The PCR amplification program	29
3.1.4.3	Gel electrophoresis for isolated DNA from <i>B. cinerea</i> fungus	31
3.1.4.4	Gel electrophoresis for PCR products	31
3.2	Tomato sampling.....	32
3.3	Infection tests of tomato by <i>B. cinerea</i>	34
3.3.1	Prepare the <i>B. cinerea</i> suspension	34
3.3.2	Tomato samples sterilization and injection	34
3.3.3	Storage condition	35
3.4	Detection the most resistance and susceptible of tomato varieties to <i>B. cinerea</i> according to time of decay	35
3.5	Visible/near-infrared spectroscopy measurement	36

3.6	Spectral data analysis	37
3.6.1	PCA analysis.....	37
3.6.2	Spectra pre-processing.....	37
3.6.3	Prediction test based on PCA models.....	38
4	Results and Discussion.....	39
4.1	Identification of <i>B. cinerea</i> fungus.....	39
4.1.1	Morphological identification	39
4.1.2	Molecular identification using a PCR.....	40
4.1.2.1	Total DNA extraction	40
4.1.2.2	Evaluation of primer to detect <i>B. cinerea</i>	40
4.2	Spectral characterization	44
4.3	PCA.....	51
4.3.1	Prediction test	56
4.4	Resistant variety to gray mold according to time decay	59
5	Conclusion and recommendation.....	61
6	Abstract in Arabic (الملخص بالعربي)	62
	References.....	65

List of Tables

Table 1. Information about the three specific primers set used to identify <i>B. cinerea</i> . Primer name, sequences, amplified bands size (bp), annealing temperature (°C) and primers concentration (nmol).....	30
Table 2. Bands amplified size by using three different specific primers to identify <i>B. cinerea</i> according to the 100 bp DNA ladder.	43

List of Figures

Figure 1. Different methods of plant disease detection (Khaled <i>et al.</i> , 2018).	10
Figure 2. The electromagnetic spectrum and NIR demonstration (Sun, 2010).	13
Figure 3. Illustration of mode for obtaining spectral data in the VIS/NIR system (El-Mesery <i>et al.</i> , 2019).	16
Figure 4. An illustration of how to separate the samples into groups using the PCA (Pasquini, 2018).	21
Figure 5. A diagram to illustrate the working principle of PCA projection (Biancolillo & Marini, 2018).	21
Figure 6. Some pictures of tomato samples infected by <i>B. cinerea</i> collected from farms near Tulkarm.	26
Figure 7. Pictures of pure <i>B. cinerea</i> fungus grown on PDA media.	26
Figure 8. Samples of three variates A: Ekram, B: Harver, C: Izmer as they collected from a local farm in Tulkarm.	33
Figure 9. Morphological characteristics of <i>B. cinerea</i> . A: spore shape under a light microscope with 4X, B: spore shape with 10X, C: spore shape with 40X, D: spore shape with oil lens.	39
Figure 10. Agarose gel electrophoresis documented photo of total DNA extracted from <i>B. cinerea</i> fungus that isolated from tomato samples using a Dneasy plant mini kit (Qiagen, cat # 69104 and 69106, Germany). Lane 1-3: DNA isolated from <i>B. cinerea</i> samples. Lane 4: negative control. M: 100 bp DNA marker ready to use (RTU).	41
Figure 11. Agarose gel electrophoresis documented photo of PCR products using three specific primer sets (C729+/C729-, BC108+/BC563- and BNTF1/BNTR1) for detection <i>B.</i>	

<i>cinerea</i> . Lane 1: specific primer set C729+/C729-. Lane 2: negative sample. Lane 3: specific primer set BC108+/BC563-. Lane 4: negative sample. Lane 5: specific primer set BNTF1/BNTR1. Lane 6: negative sample. M: 100 bp DNA marker ready to use (RTU)...42
Figure 12. A representative spectral curve of VIS/NIR (550-1100 nm) in zero-day of inoculation. Control sample (blue) and infected sample (red), with Savitzky-Golay (SG) smoothing preprocessing effect.47
Figure 13. A representative spectral curve of VIS/NIR (550-1100 nm) in the first day of inoculation. Control sample (blue) and infected sample (red), with Savitzky-Golay (SG) smoothing preprocessing effect.47
Figure 14. A representative spectral curve of VIS/NIR (550-1100 nm) in the second day of inoculation. Control sample (blue) and infected sample (red), with Savitzky-Golay (SG) smoothing preprocessing effect.48
Figure 15. A representative spectral curve of VIS/NIR (550-1100 nm) in the third day of inoculation. Control sample (blue) and infected sample (red), with Savitzky-Golay (SG) smoothing preprocessing effect.48
Figure 16. A representative spectral curve of VIS/NIR (550-1100 nm) in the fourth day of inoculation. Control sample (blue) and infected sample (red), with Savitzky-Golay (SG) smoothing preprocessing effect.49
Figure 17. A representative typical VIS/NIR (550-1100 nm) spectral curve of infected samples for all days of inoculation. Zero-day (blue), the first day (red), the second day (green), the third day (purple) and the fourth day (brown), with Savitzky-Golay (SG) smoothing preprocess.49
Figure 18. The effect of multiplicative scatter correction (MSC) preprocessing on the spectra of infected samples for all days of inoculation. Zero-day (blue), the first day (red), the second day (green), the third day (purple) and the fourth day (brown).50

Figure 19. The effect of first derivatives (1 st D) with Savitzky-Golay (SG) preprocessing on the spectra of infected samples. Zero-day (blue), the first day (red), the second day (green), the third day (purple) and the fourth day (brown).	50
Figure 20. Scores plot of PCA model based on VIS/NIR (550-1100 nm) spectra for zero-day. Control (blue) and infected (red). Two PCs explained 81% of the total variance.	52
Figure 21. Scores plot of PCA model based on VIS/NIR (550-1100 nm) spectra for the first day. Control (blue) and infected (red). Two PCs explained 74% of the total variance.	53
Figure 22. Scores plot of the PCA model based on VIS/NIR (550-1100 nm) spectra for the second day. Control (blue) and infected (red). Two PCs explained 100% of the total variance.	53
Figure 23. Scores plot of the PCA model based on VIS/NIR (550-1100 nm) spectra for the third day. Control (blue) and infected (red). Two PCs explained 99% of the total variance.	54
Figure 24. Scores plot of the PCA model based on VIS/NIR (550-1100 nm) spectra for the fourth day. Control (blue) and infected (red). Two PCs explained 99% of the total variance.	54
Figure 25. Scores plot of the PCA model based on VIS/NIR (550-1100 nm) spectra for the average of infected samples for all days. Zero-day infected (blue), the first day infected (red), the second day infected (green), the third day infected (purple) and the fourth day infected (brown). Two PCs explained 98% of the total variance.	55
Figure 26. Prediction test for unknown sample based on the PCA model for the first day for VIS/NIR (550-1100 nm). Two PCs for calibration set explained 74% of the total variance and two PCs for projection set explained 91% of the total variance.	57

Figure 27. Prediction test for unknown samples based on the PCA model for the second day for VIS/NIR (550-1100 nm). Two PCs for calibration set explained 100% of the total variance and one PC for projection set explained 99% of the total variance.	57
Figure 28. Prediction test for an unknown sample based on the PCA model for the third day for VIS/NIR (550-1100 nm). Two PCs for calibration set explained 99% of the total variance and one PC for projection set explained 99% of the total variance.	58
Figure 29. Prediction test for unknown samples based on the PCA model for the fourth day for VIS/NIR (550-1100 nm). Two PCs for calibration set explained 99% of the total variance and two PCs for projection set explained 100% of the total variance.	58
Figure 30. Illustration to compare the appearance of gray mold disease symptoms on tomato varieties to determine which ones are resistant and which are sensitive during storage days.	60

List of Abbreviations/Symbols

Abbreviation/ Notation	Details
FAO	Food and agriculture organization
VIS	Visible
NIR	Near-infrared
PCR	Polymerase chain reaction
DNA	Deoxyribonucleic acid
PCA	Principal component analysis
PLS	Partial least square
LDA	Linear discriminate analysis
PLS-DA	Partial least square-discriminant analysis
MVDA	Multivariate data analysis
MSC	Multiplication scatter correction
SNV	Standard normal variate
1 st D	First derivative
2 nd D	Second derivative
nm	Nanometer
µl	Microliter
SSC	Soluble solid content
TA	Titrateable acidity
mm	Millimeter
Km	Kilometer
m	Meter
C	Carbon
H	Hydrogen
O	Oxygen
N	Nitrogen
S	Sulfur
PC	Principal component
PDA	Potato dextrose agar
°C	Cellos degree
ml	Milliliter
rpm	Round per minute
PTUK	Palestine Technical University-Kadoorie
g	Gram
µm	Micrometer
DW	Distilled water

cm	Centimeter
A/D	Analog-to-digital
CCD	Charged coupled device
FWHM	Full width at half maximum
SG	Savitzky-Golay
Cat #	Catalog number
Rnase	Ribonuclease
KARC	Kadoorie Agricultural Research Center
min	Minute/minutes
TBE	Tris borate EDTA
UV	Ultraviolet
Ver	version
ELISA	Enzyme linked immunosorbent assay
ASTM	American society of testing and materials
MIR	Med-infrared
FIR	Far-infrared
SW-NIR	Short wavelength near-infrared
LW-NIR	Long wavelength near-infrared
R	Reflectance mode
Log 1/R	Logarithm 1/R
OLS	Olive leaf spot
AP1	Lysis buffer according to Qiagen kit
P3	Neutralization buffer according to Qiagen kit
AW1/AW2	Washing buffer according to Qiagen kit
AE	Elution buffer according to Qiagen kit
bp	Base pairs
EDTA	Ethylenediaminetetraacetic acid
nmol	Nanomolar
mM	Millimolar
Kg	Kilogram
μ M	Micromolar
RTU	Ready to use

Sensing *Botrytis cinerea* in Tomato Using Visible/Near-Infrared (VIS/NIR) Spectroscopy

Researched by: Khadija Mohammad Khames Najjar

Supervised by: Dr. Nawaf Abu-Khalaf

Abstract

Gray mold disease caused by *Botrytis cinerea* is considered one of the most common diseases that affect tomato fruits and cause economic losses; early detection of the disease can reduce 50% of the losses and increase food security. Therefore, this study aimed to employ the visible/near-infrared (VIS/NIR) spectroscopy to sense the presence of gray mold on tomato fruits in the early stages. Identify of *B. cinerea* was carried out using the polymerase chain reaction (PCR). In addition, 30 homogeneous tomato samples were collected from three different varieties, *i.e.* Harver, Izmer and Ekram, 20 samples from each variety were injected with the pathogen and 10 samples from each variety were left as a control and were measured using the VIS/NIR spectroscopy daily for five days.

Spectral data acquired from the VIS/NIR spectroscopy, with a range of 550-1100 nm, were analyzed using principal component analysis (PCA). It was found that the PCA on the second day after injection was able to distinguish

completely between infected and healthy samples before symptoms appeared, also two PCs for VIS/NIR region explained approximately 99% of the total variance in the third and fourth day. Moreover, two PCs explained 98% of the total variance for PCA that applied for the average of infected samples for all days. The PCA results showed the ability of VIS/NIR spectroscopy to detect latent infections in tomato fruits as well as the early sensing of *B. cinerea*.

Furthermore, when observing the infected samples from these varieties to detect which are resistant to gray mold disease, it was found that all of these varieties were sensitive to the disease.

1 Introduction

1.1 General introduction

Tomato (*Solanum lycopersicum* E.) is one of the most common crops in the world. According to FAO (2019), the estimated annual global production of tomato crops is 182.3 million tons. China, India and Turkey are among the most tomato producing countries in the world. The area planted with tomato in Palestine was estimated at 12.000 dunum. Accordingly, tomato crop constitutes 1.5% of total agricultural land cultivated in Palestine (ARIJ, 2015).

In recent decades, the focus has increased on the health and quality of fruits (El-Mesery *et al.*, 2019), especially agricultural products that contribute to food industries such as tomato (Cattaneo & Stellari, 2019). One of the factors that affect the quality of tomato is the presence of a pathogen that causes enormous economic losses (Hahn, 2009; Rizk, 2018).

Tomato plants infected by many pests and diseases, one of the most common diseases that affect the post-harvest tomato crop is the gray mold caused by *Botrytis cinerea* fungus (Elad *et al.*, 2007; Hennebert, 1973), which causes substantial economic losses (Petrasch *et al.*, 2019). Infected tomatoes not only cause economic losses at the level of agricultural industries but also reduce farmer's income. To reduce losses, farmers tend to use pesticides as a remedy

for the problem, which affects health in general as well as negatively affects the environment (Sannakki *et al.*, 2011).

The detection of the pathogen at the early stage of infection might help to reduce the losses, by excluding the affected fruits, thus reducing losses, especially after harvest, also reducing the use of pesticides (Khaled *et al.*, 2018).

There are many traditional methods, *i.e.* visual observation and laboratory-based methods, used to examine the quality of the fruits and to detect the pathogen. However, these methods are time-consuming, destructive and unable to detect the latent symptoms (Liu, 2016). Hence, the need for fast, environmentally friendly, non-destructive techniques that can be applied to control fruit quality has increased. One of these technologies is visible/near-infrared (VIS/NIR) spectroscopy (Cortes *et al.*, 2019a). VIS/NIR technique is the most promising alternative technology that can be applied to measure the amount of reflected, absorbed and transmitted spectra from the sample to be examined (Porep *et al.*, 2015).

This technology was used in several fields, including agricultural, industrial and others (Abu-Khalaf, 2015; Huang *et al.*, 2008; Zaid *et al.*, 2020). This method is fast, inexpensive and can be used in production lines (Wang *et al.*, 2015). On the other hand, there are still some limitations for its use, the most important of

which is the need for an expert to extract results and build a model (Cremonese *et al.*, 2019).

The ability of the VIS/NIR spectroscopy to identify and sense the pathogen in the early stages of the disease has been studied and achieved in many plants, like tomato, eggplant and wheat (Feng *et al.*, 2019; Khaled *et al.*, 2018; Shen *et al.*, 2019). To our best knowledge, there are no previous studies on the use of VIS/NIR spectroscopy with range 550-1100 nm for sensing the gray mold caused by *B. cinerea* on tomato fruits.

1.2 Aim

This study aims to test the possibility of using the VIS/NIR spectroscopy to sense the presence of *B. cinerea* in tomato in the early stage of infection.

1.3 Objectives

The objectives of this study are to:

- 1) Isolate *Botrytis cinerea*.
- 2) Sense (*i.e.* detect) the presence of *Botrytis cinerea* in tomato using VIS/NIR spectroscopy.
- 3) Detect the most resistance and susceptible variety of tomato to *Botrytis cinerea* according to time of decay.

2 Literature Review

2.1 Tomato crop importance and production

Tomato (*Solanum lycopersicum E.*) belongs to the *Solanaceae* family, is ranked the second after potatoes (*Solanum tuberosum L.*) in terms of importance (Quinet *et al.*, 2019). The global production of tomato crops distributed as follows: Asia accounts for 61.1% of global tomato production, whereas Europe produced 13.5%, America produced 13.4% and Africa produced 11.8% of the total tomato production (FAO, 2019).

The most consuming countries for tomato are China, India, North Africa, the Middle East, the USA and Brazil, where per capita consumption is estimated from 61.9 to 198.9 Kg per capita (Arah *et al.*, 2015; FAO, 2019).

Tomato contains many nutritional benefits, as it is rich in iron, citric acid, vitamin C, A and K and antioxidants, *i.e.* lycopene and carotene (FAO, 2018; Li *et al.*, 2018; Nasir *et al.*, 2015). Tomato is eaten either fresh or processed like sauce and juices (Arah *et al.*, 2015; Marti *et al.*, 2016). It also has economic importance, as the tomato industry is considered one of the most important global food industries (Viskelis *et al.*, 2015). Some factors affect the quality of tomato and cause economic losses for the crop, including infection with fungal diseases, especially after harvest. Gray mold (*Botrytis cinerea*) disease is one

of the most public diseases that affect tomato crops (Angioni *et al.*, 2012; Shi & Sun, 2017).

2.2 Food safety and quality

There is a difference between food safety and food quality, where the difference depends on the objective of the market and the application. Sometimes food safety is considered part of the food quality, but most of the time, it is difficult to judge food safety by the naked eye, given that food safety is defined as the absence of microbiological contaminants or toxic substances (Alander *et al.*, 2013).

Food quality can be defined in several ways, such as the availability of all conditions for acceptance by the consumer, but there are different conditions and standards from person to person, where the quality will be judged from a personal perspective. There is another way to define quality according to use. For example, for fresh consumption, homogeneity in size, maturity and lack of defects is considered one of the most important criteria to determine the quality. As for industrial production, colour and the absence of pathogens and pollutants that cause economic losses are essential criteria for quality (El-Mesery *et al.*, 2019; FAO, 2018; Sadilek, 2019).

The quality of fruits is determined by soluble solid content (SSC), titratable acidity (TA), firmness, appearance, flavour, nutrition value, safety and absence of pathogen (Goyette *et al.*, 2010; Huang *et al.*, 2018; Zhang *et al.*, 2019).

2.3 Gray mold

Gray mold caused by *Botrytis cinerea* fungus is considered one of the most important plant pathogens, as it was ranked among the top ten fungal pathogens infecting the plant in the world. It was in the second-order after *Magnaporthe oryzae* that causes rice blast (Dean *et al.*, 2012; Scholthof *et al.*, 2011). *B. cinerea* is an airborne plant pathogen. It belongs to the *Sclerotiniaceae* family, genus: *Botryotinia* and species: *cinerea* (Shirane *et al.*, 1988).

Botrytis cinerea can attack more than 200 plants species, *i.e.* strawberry, sweet pepper, tomato and cucumber (Elad *et al.*, 2007). It can infect different parts of the plant such as shoot, leaves, flowers and fruits (Droby & Lichter, 2007). The disease begins in the stem and leaves even in the early stages of plant growth in the green stages. Then, the spores spread to the fruits (Fillinger & Elad, 2016). Where, it can cause soft rotting in fruits and vegetables (Liu *et al.*, 2017; Mohammadi *et al.*, 2012).

The annual losses caused by *B. cinerea* were estimated at 10 billion dollars worldwide for the various crops it attacked (Weiberg *et al.*, 2013). While the

losses on the tomato crop were estimated between 15-25 million dollars (Petrasch *et al.*, 2019; Soylu *et al.*, 2010).

Culture the crops out of its season in a greenhouse increases the possibility of infection, especially tomato and cucumber crops (Gao *et al.*, 2018; Pande *et al.*, 2001). The spores need 4-6 hours to grow and infect the plant if appropriate environmental conditions are found. Cool and humid conditions (above 80%) with a moderate temperature of approximately 18-23°C are ideal for the growth and spread of *B. cinerea* spores (Elad *et al.*, 2007; Hua *et al.*, 2018).

The *B. cinerea* fungus enters the tissues in the pre-ripening stages and remains quiescent until the environmental conditions become suitable for growth. Thus, it can cause huge losses for fruits that appear healthy during the post-harvest chain (Williamson *et al.*, 2007).

Early detection of the pathogen before the appearance of symptoms is one of the most important reasons that lead to avoiding economic losses, as well as environmental protection from chemical pollutants, such as the use of fungicides (Martinelli *et al.*, 2015; Wu *et al.*, 2008).

2.4 Methods for plant disease detection

Plant disease detection in the early stages not only helps to reduce losses, but also helps to avoid the pathogen from spreading (Khaled *et al.*, 2018). Several ways are ranking from traditional to advance methods have been used to detect plant diseases (Kandpal & Cho, 2014). These methods can be divided into visual methods, laboratory-based methods and non-destructive techniques as summarized in Figure 1 (Khaled *et al.*, 2018; Rizk, 2018; Wu *et al.*, 2008).

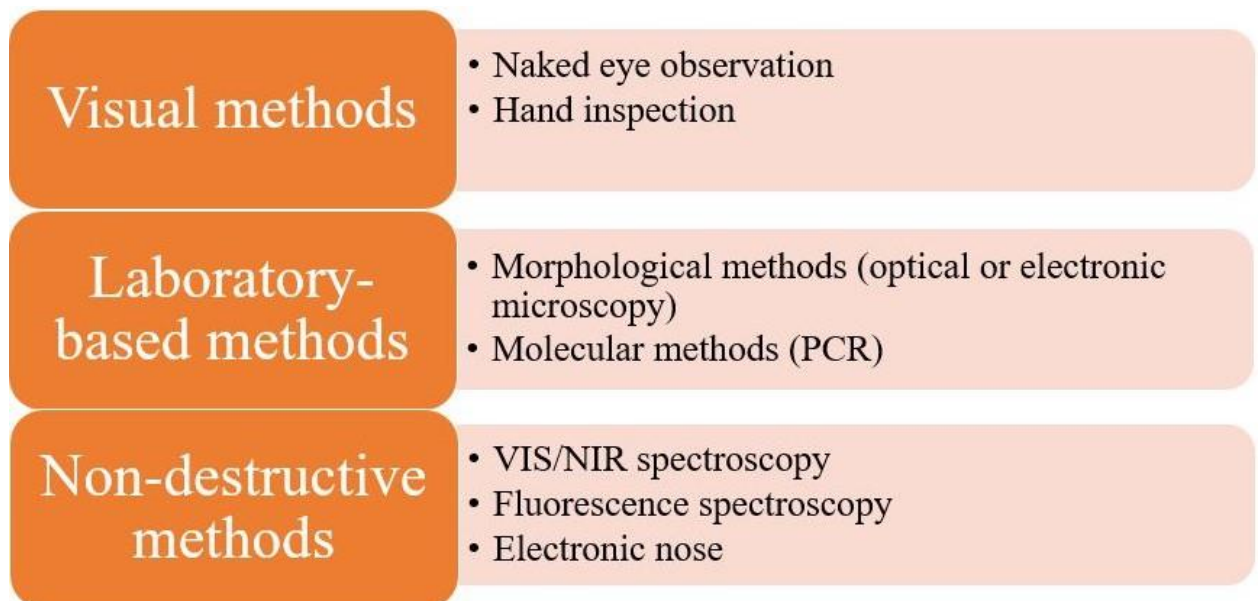


Figure 1. Different methods of plant disease detection (Khaled *et al.*, 2018).

Visual inspection is considered time-consuming, based on the appearance of fungal symptoms and inefficient to detect latent infection (Ali *et al.*, 2019). Instead, laboratory-based methods, e.g. enzyme-linked immunosorbent assay (ELISA), optical or electronic microscopy and polymerase chain reaction

(PCR), can be used as an accurate method to diagnose and detect plant diseases genetically or morphologically (Gowen *et al.*, 2007; Huang *et al.*, 2008). However, there are limitations to use these methods in early plant disease detection, such as labor-intensive and lack of rapidity for the detection of a plant pathogen. Also, these methods are destructive and expensive (Alander *et al.*, 2013; Farber *et al.*, 2019; Martinelli *et al.*, 2015).

2.4.1 Using a PCR to identify plant disease pathogens

The PCR as a molecular method has been used to identify plant disease pathogens since the 1980s (Bustin, 2017). The PCR technology replicates deoxyribose nucleic acids (DNA) by using a specific short piece of DNA called primer. The replication is carried out through three steps of different temperatures, which are repeated every cycle: the first step is denaturation step at temperature 90-95°C, the second step is annealing step at temperature 50-60°C and the final step is extension step at temperature 72°C (Harmon, 2013). The PCR is a sensitive, accurate and specific method that using in the identification of plant pathogens, like fungi, bacteria and viruses. In which, the use of a specific primer ensures accurate identification of pathogens (Fahrentrapp *et al.*, 2013; Farber *et al.*, 2019). The PCR technique has been used to identify many plant pathogens, such as *Fusarium oxysporum f.sp.*, *B. cinerea*, etc. (Harmon, 2013; Mirmajlessi *et al.*, 2015).

2.4.2 Non-destructive methods for plant disease detecting

After reviewing the drawbacks of previous methods for the detection of plant disease in the early stage, increased attention has been given to non-destructive methods to sense plant pathogens (Huang *et al.*, 2008).

Non-destructive methods such as spectroscopic technology (Saeys *et al.*, 2019), electronic nose (Wilson, 2013) and image processing techniques (Qin & Lu, 2008) have recently been used in sensing plant pathogens. These methods, including spectroscopy, have many advantages in detect plant diseases, like rapidity, simplicity, high sensitivity and can be used under field conditions (Cortes *et al.*, 2019a; You *et al.*, 2019).

Spectroscopic technology includes VIS/NIR spectroscopy (Abu-Khalaf & Salman, 2013; Abu-Khalaf *et al.*, 2004), mid-infrared absorption (Zhang *et al.*, 2017), Raman scattering (Lee *et al.*, 2013), nuclear magnetic resonance (NMR) (Martinelli *et al.*, 2015), microwave absorption (Sun, 2010) and ultra-sound transmission (El-Mesery *et al.*, 2019) have been applied to detect plant diseases in the early stage.

2.4.2.1 Visible/near-infrared spectroscopy

According to the American Society of Testing and Materials (ASTM), the visible (VIS) spectrum covers the wavelength range of 400-750 nm, near-infrared (NIR) covers the wavelength range of 780-2500 nm, mid-infrared

(MIR) of 2500-25,000 nm and far-infrared (FIR) of 25,000-100,000 nm as shown in Figure 2 (Khaled *et al.*, 2018; Pasquini, 2018).

NIR contains two important regions, short-wavelength (SW-NIR) with range 750-1300 nm and long-wavelength (LW-NIR) with range 1300-2500 nm (Mahlein *et al.*, 2010).

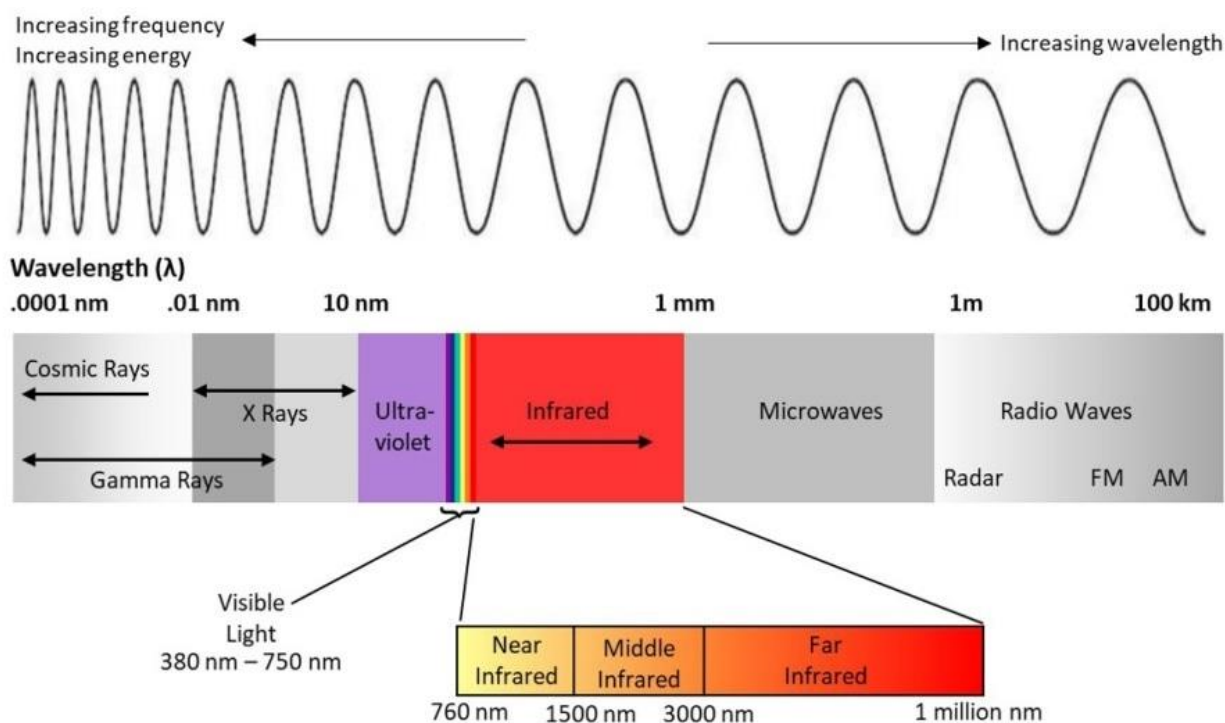


Figure 2. The electromagnetic spectrum and NIR demonstration (Sun, 2010).

The principle of the VIS/NIR action is based on molecular vibration between C-H, O-H, S-H and N-H bonds of the main compounds (water, sugars, chlorophylls, carotenoids, etc.), which caused by photon absorption (Kandpal & Cho, 2014; Kumaravelu & Gopal, 2015). A photon can be absorbed only if it

has the proper energy to stimulate one of the vibrational states of the molecule. Though, the fundamental vibrations of these bonds occur in the infrared region; therefore, the absorption in the VIS/NIR region is caused by overtones and combinations of these fundamental vibrations. Where this yields absorption peaks in the VIS/NIR region that are wide-ranging and overlapping (Nicolai *et al.*, 2014). At room temperature, organic compounds remain in continuous motion (Teye *et al.*, 2013). When these particles are exposed to electromagnetic energy, they absorb energy that is proportional to fractionation mode (Beghi *et al.*, 2017).

Because each material differs in its components from the other, the resulting spectrum is unique and distinct to each material. So, the VIS/NIR technology can be considered a fingerprint (spectral signature) technique, that allows applying in detect plant disease (Marin-Ortiz *et al.*, 2020; Qu *et al.*, 2015; Wang *et al.*, 2015).

The VIS/NIR spectroscopy can be applied in three different modes, they are reflectance, transmittance and interactance. The main difference between them is the location of the detector to the light source as shown in Figure 3 (Nicolai *et al.*, 2014).

Reflectance mode is applied to obtain information about the fruit surface. It is considered as the easiest mode because it does not need to touch the fruit and has high energy that may reach 80% (Abu-Khalaf *et al.*, 2004). Nevertheless, it is sensitive to the properties of the surface of the fruit, which affects the measurements. As for the location of the detector and the light source, they are located on the same side (Ncama *et al.*, 2018; Schaare & Fraser, 2000). While the transmittance mode is suitable for obtaining internal information of the fruit and is considered less sensitive compared to reflectance. However, the amount of light penetrating the fruit is small. The location of the detector and the light source are located opposite each other (Liu, 2016).

Lastly, interactance mode is used to obtain internal and external information of the fruit. As for the location of the detector and the light source, they are located in parallel to each other (Khaled *et al.*, 2018; Xu *et al.*, 2009). The appropriate mode is chosen based on the aim of the study. However, reflectance mode (R) are usually applied and later converted to absorption ($\log 1/R$) for later analysis (He *et al.*, 2005; Zude, 2008).

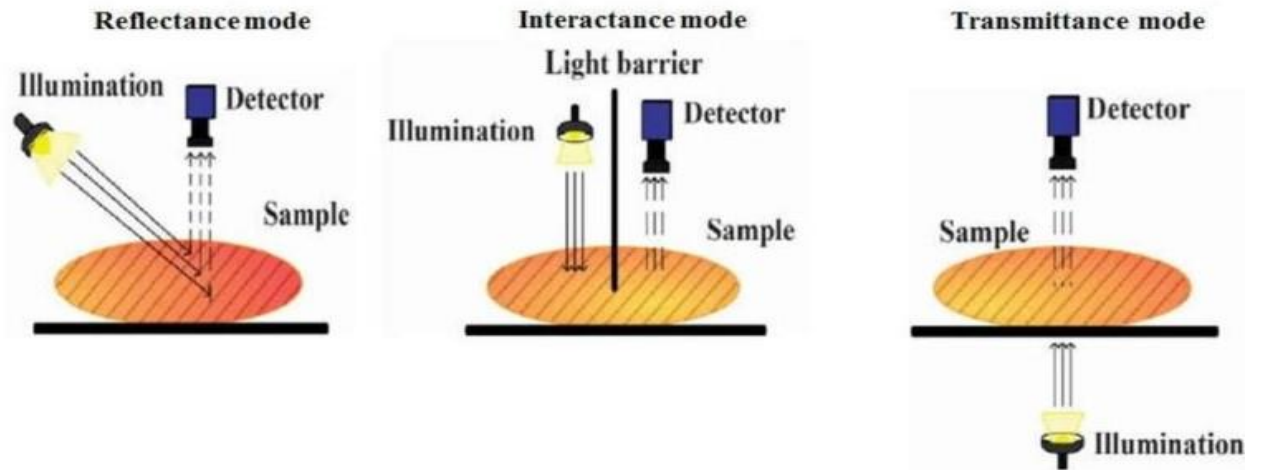


Figure 3. Illustration of mode for obtaining spectral data in the VIS/NIR system (El-Mesery *et al.*, 2019).

The VIS region contains information about fruit pigments, like chlorophyll and carotenoids. While the NIR region gives more information about the water, protein and carbohydrate content of fruits. Thus, the combination of these two regions is better for obtaining accurate results for fruit examination (Butz *et al.*, 2005; Fahrentrapp *et al.*, 2019; Khaled *et al.*, 2018).

2.4.2.2 Visible/near-infrared spectroscopy applications

The VIS/NIR technique has been used since the 1800s, as Frederick William Herschel was the first to use it (Alander *et al.*, 2013). Furthermore, in recent decades, its use has increased (Farber *et al.*, 2019). For example, it was used in several fields, including quality control of fruits and vegetables (Abu-Khalaf & Bennedsen, 2004; Farres *et al.*, 2019; Nicolai *et al.*, 2007), additionally using portable VIS/NIR spectroscopy to control the quality of fruits (Dos Santos *et al.*, 2013; Skolik *et al.*, 2019). Also, VIS/NIR spectroscopy was used for the identification of nutrients in the plant (Sharon Ruth *et al.*, 2018). Likewise, it was used in the fields of livestock (Bahri *et al.*, 2019), the identification of microbiological contaminants in meat (Feng & Sun, 2013), also is used in soil studies (Dos Santos *et al.*, 2013). Moreover, it was used in the fields of medicine and drug manufacturing (Luypaert *et al.*, 2007). Many studies published in the field of using VIS/NIR technique in agricultural industries to control the quality of fruits for more than one application, such as off-line, at-line, on-line and in-line measurements (Cortes *et al.*, 2019a; Ncama *et al.*, 2018; Nicolai *et al.*, 2014). The differences between these terms are as follows (Cortes *et al.*, 2019b; Dickens, 2010):

Off-line: checks are carried out in the laboratory away from production lines.

At-line: samples testing in a place very close to production lines, where random samples are chosen manually for testing.

On-line: samples are selected from production lines and converted into a recycling loop for testing and return to production lines.

In-line: analysis of samples within production lines (in situ).

2.4.2.3 Visible/near-infrared technology advantages and limitations

The VIS-NIR technology has several advantages when compared to traditional methods; it is non-destructive, fast, does not need to prepare samples, robust method (El-Mesery *et al.*, 2019), suitable for in-line and on-line mentoring (Rizk, 2018), real-time analysis and suitable for checking physical and chemical properties (Kumaravelu & Gopal, 2015). It can also be used to check hazardous materials (Beghi *et al.*, 2017), as well as suitable for examining the intrinsic properties of agricultural commodities (Wang *et al.*, 2015). Moreover, it is an environmentally friendly technology (Garcia-Sanchez *et al.*, 2017). On the other hand, there are some limitations to its use. It needs an expert, because it depends on the multivariate data analysis (MVDA) to extract the results, the model construction needs many different samples. Nevertheless, these problems can be overcome through data analysis (Brereton *et al.*, 2017; El-Mesery *et al.*, 2019). The temperature may affect the accuracy of the measurement (Peirs *et*

al., 2003) and it needs a reference in the case of quality analysis (Nicolai *et al.*, 2007).

2.4.2.4 Visible/near-infrared spectral data analysis

The VIS/NIR spectra acquired contain a large number of data that need to be analyzed to extract useful information from it (Farres *et al.*, 2019; Qu *et al.*, 2015). So that, chemometrics (a combination between mathematical and statically science) also called MVDA is considered the best way to analyze such data complex (Amigo *et al.*, 2013; Brereton *et al.*, 2017).

2.4.2.4.1 Multivariate data analysis (MVDA)

Multivariate data analysis (MVDA) is a powerful method for extracting results and useful information (Kumar & Sharma, 2017). It is defined as a mathematical tool that relies on statistical equations to analyze the data (Hair *et al.*, 1998). MVDA includes a variety of methods for spectral data analysis, like preprocessing and building calibration models for qualitative and quantitative analysis (Beghi *et al.*, 2018). Principal component analysis (PCA) (Guifang *et al.*, 2015), partial least squares (PLS) (Kawamura *et al.*, 2017), linear discrimination analysis (LDA) (Baranowski *et al.*, 2012) and partial least squares-discriminant analysis (PLS-DA) (Cen *et al.*, 2007) are commonly applied for spectral analysis. Many software programs are used for data

analysis, such as the Unscrambler program (Abu-Khalaf & Salman, 2013; Zaid *et al.*, 2020).

2.4.2.4.2 Principal component analysis (PCA)

Principal component analysis (PCA) is a bilinear mathematical method and is also known as a projection method (Wold *et al.*, 1987). PCA model aims to extract information from spectral data (X matrix) and ignore the noise (Farres *et al.*, 2019). The X matrix has many numbers of components called principal component (PC), which is calculated according to the following equation (Biancolillo & Marini, 2018):

$$X=TP^T+E$$

Where T is scores matrix, P the loading matrix and E the error matrix

Each PC gives information about the variables. The first PC has the most information and the last one has the least information (Rady *et al.*, 2018). The PCA analysis is used to distinguish between measured variables, through which groups can be made of samples and explain the extent of similarity and difference between samples, as shown in Figure 4 (Morawski & Mi-Okina, 2016). An illustration of the PCA working principle is shown in Figure 5.

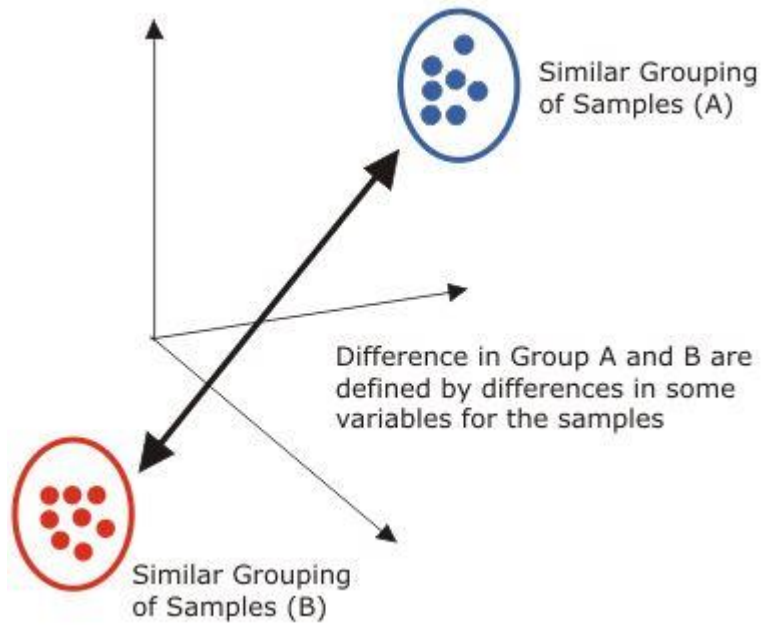


Figure 4. An illustration of how to separate the samples into groups using the PCA (Pasquini, 2018).

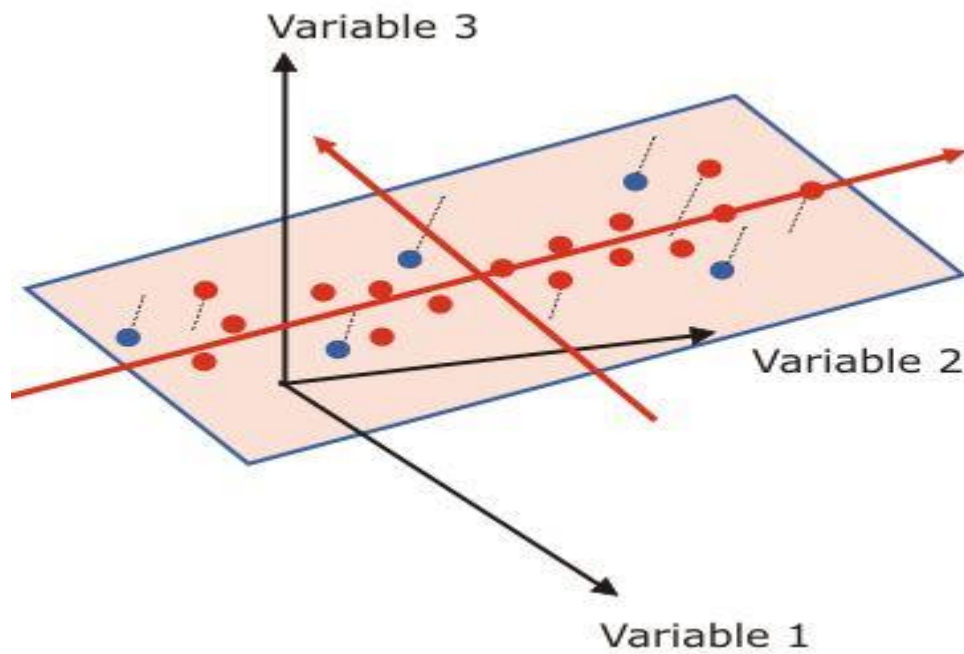


Figure 5. A diagram to illustrate the working principle of PCA projection (Biancolillo & Marini, 2018).

2.4.2.4.3 Pre-processing of spectral data

During the measurement, spectral data may be influenced by internal factors, such as the occurrence of drift, or it may be affected by external factors, such as heat, and these factors may cause missing some information and make high noise in acquired spectra. Therefore, some preprocessing methods are needed to obtain accurate results (Geladi *et al.*, 1985; Wei *et al.*, 2016). In which, Savitzky-Golay (SG) smoothing is the most commonly used to remove high noise from the acquired spectra (Savitzky & Golay, 1964). Moreover, multiplicative scatter correction (MSC), which is used to remove slope variation and correct the effect of random scattering (Isaksson & Naes, 1988). Standard normal variate (SNV) is another technique that can be applied with the MSC or alone to correct the scattering effect (Barnes *et al.*, 1989; Steinier *et al.*, 1972). Also, first (1st D) and second (2nd D) derivatives can be applied with Savitzky-Golay transformation to reduce drift and scattering, respectively (Karstang & Manne, 1992; Liu *et al.*, 2010; Sun, 2010). These methods can be applied alone or combined to obtain the best results (Wang *et al.*, 2015).

2.5 Visible/near-infrared spectroscopy application for plant diseases detection

The ability of the VIS/NIR spectroscopy technique to distinguish between infected and healthy plants was investigated (Hahn, 2009; Rizk, 2018; Saeys *et al.*, 2019; Sharon Ruth *et al.*, 2018). Many studies have applied VIS/NIR spectroscopy technology for detecting plant diseases at an early stage. Examples of these diseases, *B. cinerea* on eggplant leaves (Wu *et al.*, 2008), fire blight disease on pome fruit (Bagheri & Mohamadi-Monavar, 2020) and olive leaf spot (OLS) on olive leaves (Abu-Khalaf & Salman, 2013).

Moscetti *et al.* (2015) tested the ability of VIS/NIR spectroscopy with a range of 400-2500 nm to detect bactrocera olea that infested olive fruit and they could build a PCA model that explained 98% of the total variance for distinguishing between infected and healthy samples. Likewise, Sankaran *et al.* (2012) applied the VIS/NIR technique with a range of 350-2500 nm to detect laural wilt disease on avocado leaves. The results of this study showed the ability of VIS/NIR spectroscopy to differentiate between healthy and unhealthy samples, where the accuracy of the PCA model was 80%.

Moreover, Bienkowski *et al.* (2019) studied the possibility of VIS/NIR spectroscopy with a range of 400-1000 nm to detect late blight disease on potato plants. In their study, the PCA model with accuracy 92% could distinguish

between infected and uninfected samples. Furthermore, the VIS/NIR spectroscopy with a range of 380-2500 nm was investigated to early sensing of *Fusarium oxysporum* fungus on tomato leaves, where the PCA model with 100% could distinguish between healthy and unhealthy samples (Marin-Ortiz *et al.*, 2020).

In addition, Wu *et al.* (2008) used VIS/NIR reflectance spectroscopy with range 400-1100 nm to early detect of *B. cinerea* fungus that affects eggplant leaves. The results of PCA showed the ability of the VIS/NIR spectroscopy to detect the disease before symptoms appear, where it was able to classify infected and healthy samples in the second day of injection with an accuracy of 80%.

These studies showed the possibility of using the VIS/NIR technique with a range of 400-2500 nm to sense plant pathogens, especially in the early stages. However, few studies have been published on the application of MIR with a range of 2500-25,000 nm for plant disease detection. The reason may be due to the high cost and complexity of MIR spectroscopy (Khaled *et al.*, 2018).

3 Materials and Methods

3.1 Fungal methods

3.1.1 Media preparation

Potato dextrose agar (PDA) media has been prepared in Kadoorie Agricultural Research Center (KARC) laboratories according to the manufacturer instructions available on the bottle (Difco laboratories, USA) (cat # 254920). Where, 31.2 g of PDA powder dissolved in 800 ml of distilled water (DW), autoclaved at 121°C for 1 h. After that, the media was left to cool for 15 min, then poured in sterile petri-dishes (9 cm) and it was left to solidify. Subsequently, it was stored at 4°C for *B. cinerea* fungus isolation.

3.1.2 Isolation and identification of the fungi

Samples of tomato infected with gray mold disease were collected from farms in Tulkarm (Figure 6). A small portion of the sample was placed over fresh PDA media, closed with parafilm, labelled and incubated at 22±1°C (Borges *et al.*, 2014). Pure fungal cultures were obtained by several sterile transfers of the colony growth to fresh PDA media. The *B. cinerea* fungus was subcultured on fresh PDA media every two weeks, by culturing 4 discs from old cultured growth on fresh PDA media were kept in an incubator at 22±1°C to get full growth (Figure 7).



Figure 6. Some pictures of tomato samples infected by *B. cinerea* collected from farms near Tulkarm.

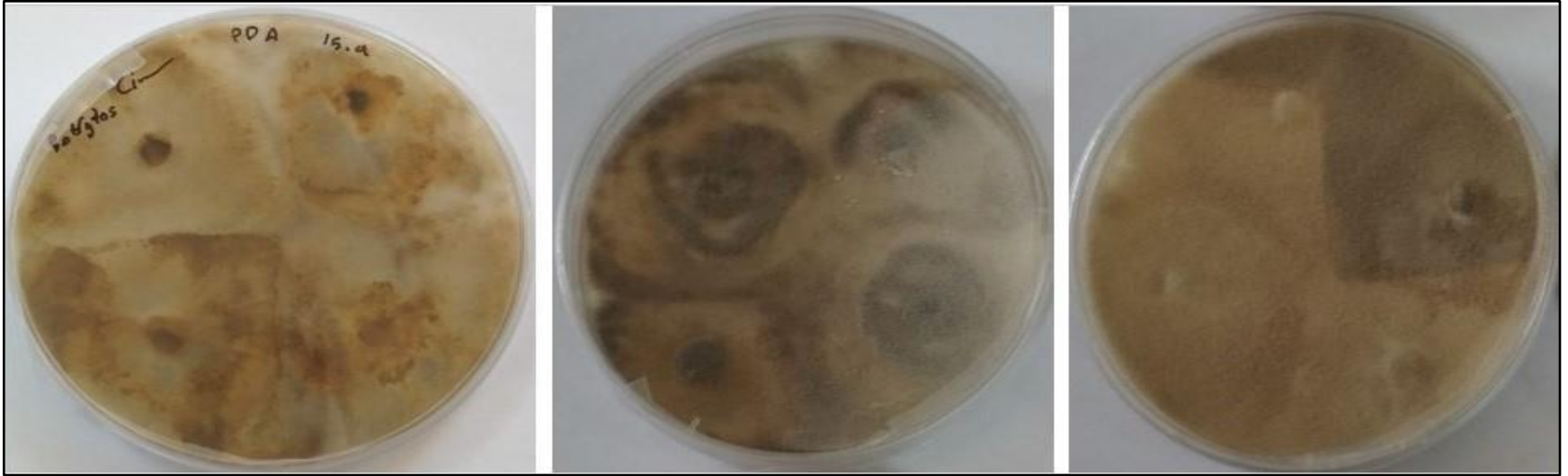


Figure 7. Pictures of pure *B. cinerea* fungus grown on PDA media.

3.1.3 Morphological identification

The morphological characteristics of the *B. cinerea* were studied based on the shape of fungal spores and conidia color (Elad & Shtienberg, 1995). For this purpose, after 14 days of incubation, a small portion of fungus was used to prepare a microscopic slide and observed by a light microscope (Labomed, USA) (cat # PN: 9135000-901). Images were recorded with an Aiptekhd1080P digital camera (Aiptek International GmbH, Germany).

3.1.4 Molecular identification

3.1.4.1 Fungal DNA extraction

The fungal DNA was extracted following a Dneasy plant mini kit (Qiagen, Germany) (cat # 69104 and 69106). Briefly, 60-100 mg of seven days grown fungi were scratched from PDA surface media using a sterile scalpel and were placed in a sterile 1.5 milliliter microfuge tube. About 400 µl lysis buffer (AP1) (cat # 154053337) was added to each tube. Tubes content was ground and homogenized using pellet pestles cordless motor (Sigma-Aldrich, Z359971-1EA, Germany) (cat # 3110) with sterilized tips, then 4 µl of RNase (cat # 154052147) were added to each tube. After that, the microfuge tubes were incubated at 65°C water bath for 10 min with gently shaking for 2 times during incubation. Then, 130 µl of neutralization buffer (P3) (cat # 154043250) was added and placed the tubes in ice for about 5 min. Tubes were centrifuged for 5

min at 14000 round per minute (rpm). The lysate was transferred into a sterile 2 ml collection tube. Then, the tubes were centrifuged for 2 min at 14000 rpm. Afterward, the flow-through was transferred to a new microfuge tube and added 1.5 of the transferred volume from washing buffer 1 (AW1) (cat # 15405097) and mixing gently. Then, 650 µl of the mixture was transferred to the DNase mini spin column placed in a new 2 ml collection tube and centrifuged for 1 min at 8000 rpm followed by removed the flow through. The spin-column was placed in a new 2 ml collection tube and 500 µl of washing buffer 2 (AW2) (cat # 15705041) was added and centrifuged for 1 min at 8000 rpm. The spin-column was transferred to a new 1.5 ml microfuge tube with added 100 µL of elution buffer (AE) (cat # 154050916). Then the tubes were left for 5 min at room temperature 25°C and centrifuged for 1 min at 8000 rpm. In the end, the tubes were kept at -20°C for further use after checking the DNA using gel electrophoresis (Rigotti *et al.*, 2002).

3.1.4.2 Polymerase chain reaction (PCR)

The *B. cinerea* was identified by PCR using three different specific primers sets which are C729+/C729-, which was designed to specifically distinguish *B. cinerea* from other Botrytis species and other fungi, where this primer was used to amplify 700 bp of *B. cinerea* DNA fragment (Rigotti *et al.*, 2002). BC108F/BC563R primer set was designed to amplify internal DNA fragment

500 bp of *B. cinerea* species (Fan *et al.*, 2015; Rigotti *et al.*, 2006). BNTR1/BNTF1 primer pair that designed to detect small fragments of DNA 112 bp for *B. cinerea* DNA (Song *et al.*, 2008). First, the primers were prepared, where DNase free water was added to obtain 100 μ M concentration. PCR was performed in a 25 μ l reaction mixture for each primer pair. Each mixture containing 12.5 μ l of 2X GoTaqVR Green Master Mix (Promega Corporation, USA) (cat # 0000382528), 0.2 μ l forward primer, 0.2 μ l reversed primer, 1 μ l Fungal DNA and 11.1 μ l from ultra-pure DNase free water (Biological Industries, cat # 1710266, USA). One PCR mixture without any template DNA was used as a negative control.

3.1.4.2.1 The PCR amplification program

The amplification program was performed using Verti™ 96 well thermal cycler (cat # 4375786) (Applied Biosystems Company, California, USA), programmed to perform an initial denaturation cycle at 94°C for 2 min, then 35 cycles of 94°C for 45 sec, the annealing step for different primer combination (Table 1) for 50 sec, and 72°C for 50 sec and the final cycle at 72°C for 5 min. To ensure the reproducibility of the DNA amplified fragments, all PCRs were triplicated for each primer pair.

Table 1. Information about the three specific primers set used to identify *B. cinerea*. Primer name, sequences, amplified bands size (bp), annealing temperature (°C) and primers concentration (nmol).

Primer	Sequences (5'-3')	Band size (bp)	Annealing temperature (°C)	Concentration (nmol)	reference
C729+ (cat # 4425691)	(AGCTCGAGAGAGATCTCTGA)	700-750	50	19.1	(Gindro <i>et al.</i> , 2005)
C729- (cat # 4425692)	(CTGCAATGTTCTGCGTGGAA)			19.5	
BC108+ (cat # 4425695)	(ACCCGCACCTAATTCGTCAAC)	500-600	55	21.1	(Rigotti <i>et al.</i> , 2006)
BC563- (cat # 4425690)	(CTGCAATGTTCTGCGTGGAA)			19	
BTNF1 (cat # 4425693)	(GCTTGACCCAGGCTTGAAC)	112	50	21	(Song <i>et al.</i> , 2008)
BTNR1 (cat # 4425694)	(TGGGTCTGGTCCCGTGTA)			17.2	

3.1.4.3 Gel electrophoresis for isolated DNA from *B. cinerea* fungus

The isolated DNA running on 1.5% agarose gel. The gel was prepared by weighing 1.5 g of agarose powder and it was completely dissolved in 100 ml of 0.5x Tris-borate-ethylenediaminetetraacetic acid (EDTA) (TBE) buffer using the microwave. After that, the mixture was cooled at room temperature, then 4 μ L of 1000 x gel red DNA stain (cat # 41003) was added with moving. The mixture was poured in a tray (20*20 cm) of the Submarine Horizontal type electrophoresis system. After that, 10 μ l of the DNA with 2 μ l of a blue orange loading dye 6x (cat # 043043) and 2.5 μ l of 100 bp molecular marker ready to use (RTU) (cat # DM003-R500) were loaded carefully in a well of solidified gel. The device (Helixx Mupid- exU, USA) was run for 60 min at 70 volts. After that, the DNA was viewed under ultraviolet (UV) illuminator device (Uvitec, cat # 1210234, Cambridge) and gel documentation system.

3.1.4.4 Gel electrophoresis for PCR products

The gel was prepared by weighing 2 g of agarose powder that dissolved in 100 ml of TBE buffer using the microwave. After that, 4 μ l of 1000x gel red was added and the suspension was poured in (20*20) tray of the Submarine Horizontal type. Then, 5 μ l of PCR products was loading and 2.5 μ l of 100 bp DNA RTU ladder (cat # DM003-R500) was used as a molecular marker. The

device was run for 3 h at 70 volts. Then, the bands were viewed and documented using SynGene gene tool system (Synoptics Ltd., Cambridge C, UK) for image gaining and documentation. Besides, the PCR products were analyzed using gel SynGene Ver. 4.3.5 (Synoptics Ltd., Cambridge C, UK) analysis software to determine the molecular weight of bands.

3.2 Tomato sampling

Samples were collected according to the recommendation of the Tulkarm Agriculture Directorate. Ninety tomato samples of three local varieties (*i.e.* Harver, Izmer and Ekram), each variety has 30 samples were collected from a farm in Tulkarm, Palestine. Tomato crop was grown in a greenhouse with standard cultivation parameters. The samples were harvested free from disease or defects and with 70% maturity as shown in Figure 8 (Feng *et al.*, 2019). All samples were approximately homogeneous in size (Abu-Khalaf, 2015). The samples were placed in cardboard boxes and transferred directly to KARC laboratories, where they were stored at room temperature of $25\pm 1^{\circ}\text{C}$ for further process.



Figure 8. Samples of three variates A: Ekram, B: Harver, C: Izmer as they collected from a local farm in Tulkarm.

3.3 Infection tests of tomato by *B. cinerea*

3.3.1 Prepare the *B. cinerea* suspension

The fungus suspension was prepared according to Zhang *et al.* (2014) protocol. Where, fourteen days after cultured the fungi, the spores were harvested by immersing the culture with KH_2PO_4 -glucose solution (0.43 g of KH_2PO_4 (10 mM), 0.495 g of glucose (10 mM) and 125 μl of Tween-80 for 250 ml) for 5 min with gently moving the surface by a sterile glass rod. Then, the suspension was filtered using two layers of cheesecloth and placed in a sterile 50 ml test tube, this step was repeated more than once to ensure the most significant number of spores are obtained. Then the concentration of spores was adjusted to 5×10^4 per ml under the optical microscope (Labomed, USA) (cat # PN: 9135000-901) using a hemocytometer.

3.3.2 Tomato samples sterilization and injection

The collected tomato samples were immersed with a 2% sodium hypochlorite (NaOCl) for 2 min. Then it was washed with sterile DW. After that, samples were left to dry at room temperature for 2 h. Then, 20 samples of each variety were inoculated with the spore's suspension (the suspension mixed by Vortex before using). Four wounds were made in each fruit in the area close to the neck, where 10 μl were injected into each wound using a sterile needle. Control samples (*i.e.* 10 samples of each variety) were injected with KH_2PO_4 solution,

where 10 µl were injected into each one of four wounds made in each fruit. This method of sterilization and injection has been applied as described by Borges *et al.* (2014) and Zhang *et al.* (2014).

3.3.3 Storage condition

The samples were examined daily using VIS/NIR spectroscopy, where the samples (infected and control) were stored in plastic containers (30 * 22 cm) and covered with plastic film. Samples were sprayed with sterile DW to provide adequate moisture (about 90% relative humidity, which is optimal to *B. cinerea*) after each examination and were kept at 25±1°C (Borges *et al.*, 2014).

3.4 Detection the most resistance and susceptible of tomato varieties to *B. cinerea* according to time of decay

To determine differences in resistant to the pathogen among the three varieties (*i.e.* Harver, Izmer and Ekram), incubated samples with the *B. cinerea* were daily monitored for five days of incubation successively.

3.5 Visible/near-infrared spectroscopy measurement

The VIS/NIR spectroscopy with a USB 2000+ miniature fiber optic spectrometer (Ocean Optics, USA), Vivo light source and 50 μm fiber optics probe was used for sensing *B. cinerea*. A spectra range for VIS/NIR spectroscopy 550-1100 nm and a resolution of 0.35 nm full width at half maximum (FWHM). Besides, it has a 2-MHz analog to digital (A/D) converter, a 2048-element CCD-array detector, also a high-speed USB 2.0 port. Vivo system has four tungsten-halogen bulbs, and this allows the user to use one or more bulbs. The four halogen tungsten light sources make the Vivo a high-powered VIS/NIR source, which allows a shorter integration time than conventional methods (Ocean Optics, USA). To avoid the risk of overheating the sample, this device equipped with a capable cooling fan. The USB2000+ can be controlled by Spectra Suite software. Tomato samples (infected and healthy samples) were measured for each variety daily for five days (*i.e.* zero-days, first day, second day, third day and fourth day of inoculation). The integration time used in every day was 300 μs . Each sample was examined three times, to confirm the stability of the spectra, and then the average was taken for the three measurements. The VIS/NIR analyses were done in the diffuse reflectance mode and then recorded as absorbance (*i.e.* $\log(1/R)$). A diffuse reflectance standard for the system was used every 10 samples during the

experiment to ensure the stability of the measurement. The calibration of the light was done in the beginning by closing the entrance of incoming light from a fiber probe to the USB2000+ miniature fiber optic spectroscopy using a plastic cap. At the end of all measurements, the acquired spectra were stored for a later process, where the measurements were carried out at room temperature $25\pm 2^{\circ}\text{C}$ and with relative humidity 60% according to the recommendation of manufacture.

3.6 Spectral data analysis

The Unscrambler program (version 10.4, CAMO Software AS, Oslo, Norway) was used for spectral data analysis.

3.6.1 PCA analysis

To study the ability of VIS/NIR spectroscopy to distinguish between infected and control samples in the early stage of *B. cinerea* growth, PCA models were carried out for VIS/NIR region (550-1100 nm).

3.6.2 Spectra pre-processing

Different pre-processing techniques for raw data were carried out before plotting the spectra curve, such as SG smoothing, MSC and 1stD (Carlos *et al.*, 2019).

3.6.3 Prediction test based on PCA models

After establishing the PCA models, new tomato samples were collected to check the ability of the PCA model to predict new samples. Where some of them were injected with *B. cinerea* in the same way mentioned in this study and others were left as a control. After that, the samples were examined using the VIS/NIR spectroscopy daily, starting from the first day of the injection (*i.e.* after 24 h).

4 Results and Discussion

4.1 Identification of *B. cinerea* fungus

4.1.1 Morphological identification

The *B. cinerea* was identified morphologically, as shown in Figure 9. Where results obtained were similar to previous studies that defined the *B. cinerea* based on the spore shape using an optical microscope (Leyronas *et al.*, 2012; Sharma & Pandey, 2010; Takam *et al.*, 2019; Williamson *et al.*, 2007).

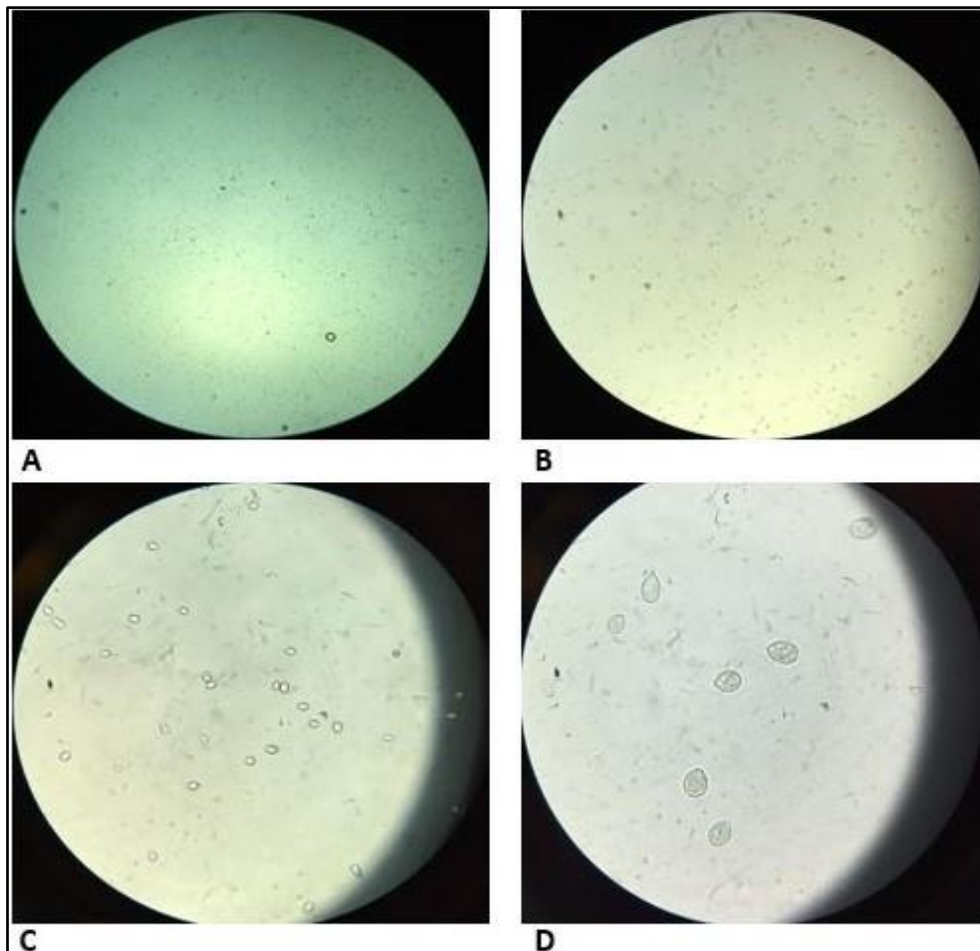


Figure 9. Morphological characteristics of *B. cinerea*. A: spore shape under a light microscope with 4X, B: spore shape with 10X, C: spore shape with 40X, D: spore shape with oil lens.

4.1.2 Molecular identification using a PCR

4.1.2.1 Total DNA extraction

The total DNA extracted from *B. cinerea* isolates is shown in Figure 10 using a Dneasy plant mini kit (Qiagen, Germany). The results showed the presence of an amount of DNA in the three samples that were isolated from it, while nothing appeared in the negative sample.

4.1.2.2 Evaluation of primer to detect *B. cinerea*

Results from three specific primers set PCR assays indicated that the primers set (C729+/C729-, BC108+/BC563- and BNTF1/BNTR1) exhibited high specificity in detecting *B. cinerea* as shown in Figure 11. The primer set C792+/- generated fragment approximately 700 bp in DNA isolated fungal samples from tomato, indicating that the isolate was *B. cinerea* as confirmed by Rigotti *et al.* (2002). Also, the primer set BC108+/BC563-, which was designed to identify *B. cinerea*, amplified a 599 bp fragment from DNA isolated fungal, conforming that the isolates were *B. cinerea* (Fan *et al.*, 2015; Narayanasamy, 2010; You *et al.*, 2019). Besides, the primer pair BNTF1/BNTR1, which was designed to amplify an internal fragment for *B. cinerea* generated approximately 110 bp fragments in DNA isolated samples (Song *et al.*, 2008). In all PCRs no generated in negative samples. In addition, the molecular weight of bands was determined using SynGene software program Ver. 4.3.5

(Synoptics Ltd., Cambridge C, UK) as shown in Table 2. These results are in agreement with previous studies (Rigotti *et al.*, 2002; Rigotti *et al.*, 2006; Song *et al.*, 2008).

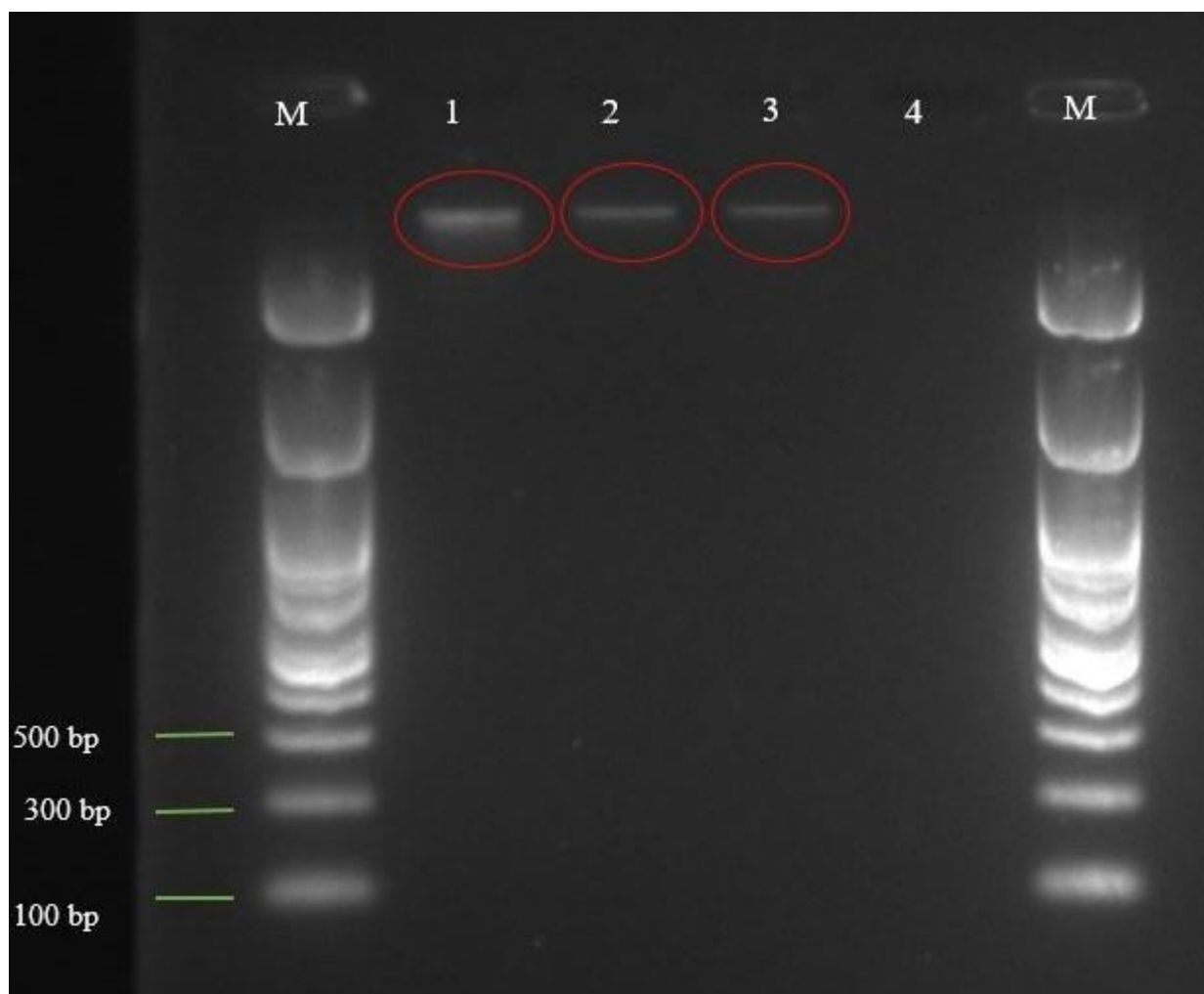


Figure 10. Agarose gel electrophoresis documented photo of total DNA extracted from *B. cinerea* fungus that isolated from tomato samples using a Dneasy plant mini kit (Qiagen, cat # 69104 and 69106, Germany). Lane 1-3: DNA isolated from *B. cinerea* samples. Lane 4: negative control. M: 100 bp DNA marker ready to use (RTU).

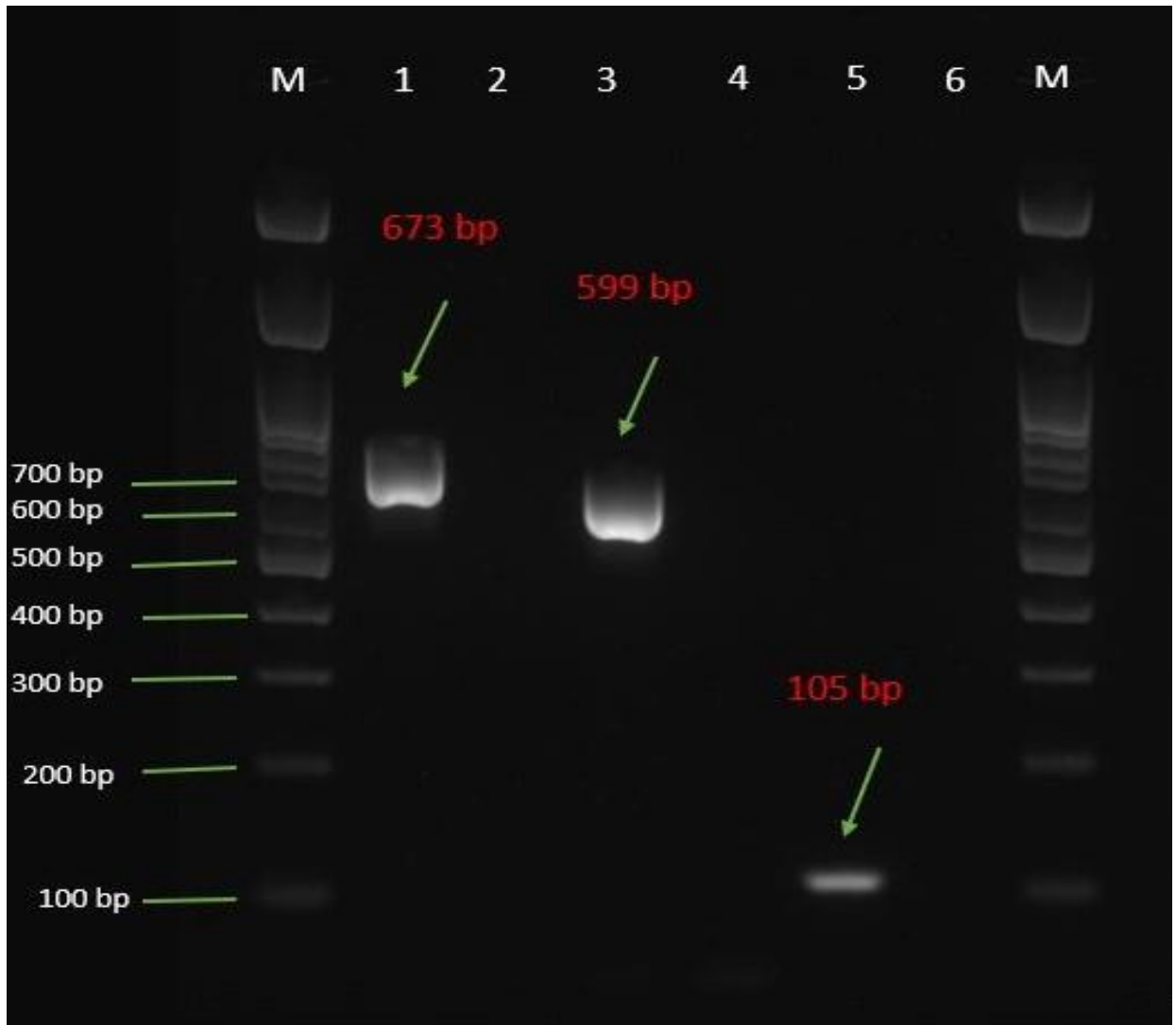


Figure 11. Agarose gel electrophoresis documented photo of PCR products using three specific primer sets (C729+/C729-, BC108+/BC563- and BNTF1/BNTR1) for detection *B. cinerea*. Lane 1: specific primer set C729+/C729-. Lane 2: negative sample. Lane 3: specific primer set BC108+/BC563-. Lane 4: negative sample. Lane 5: specific primer set BNTF1/BNTR1. Lane 6: negative sample. M: 100 bp DNA marker ready to use (RTU).

Table 2. Bands amplified size by using three different specific primers to identify *B. cinerea* according to the 100 bp DNA ladder.

Track 1			Track 2			Track 3			Track 4		
Mol. weight	Height	Quantity	Mol. weight	Height	Quantity	Mol. weight	Height	Quantity	Mol. weight	Height	Quantity
3000	1.198	40									
1500	31.224	70									
1000	20.243	50									
900	22.035	40									
800	7.019	40									
700	6.684	30	673.755	90.182	126.41						
600	7.763	30				599.373	96.596	143.23			
500	25.583	90									
400	32.412	40									
300	31.154	30									
200	21.212	40									
100	18.492	40							105.126	87.311	104.53

Track 1: molecular size marker (100 bp DNA ready to use ((RTU) ladder, cat # DM003-R500).

Track 2: band from specific primer set C729+/C729-.

Track 3: band from specific primer set BC108+/BC563-.

Track 4: band from specific primer set BNTF1/BNTR1.

4.2 Spectral characterization

Representative samples were chosen and the spectra curves were carried out for VIS/NIR region with a range of 550-1100 nm. Because the acquired spectra are affected by external factors *i.e.* heat, as well as the properties of the fruit itself, which leads to noise. It was necessary to apply some preprocessing methods before plotting the spectra curves. Savitzky-Golay (SG) smoothing was carried out as a first step (Mogollon *et al.*, 2019).

When the fruits are infected, some internal and external changes occur as a result of the growth of the fungus or pathogen. These changes make the spectra acquired from the healthy sample differ from the affected sample. This confirms that VIS/NIR spectroscopy works as a fingerprint. Therefore, there was no difference between the spectra of the infected and healthy samples in zero-day of injection as shown in Figure 12.

Whereas, in the first day and second day, *i.e.* 24-48 hours after injection, where internal changes (*e.g.* water content and carbohydrate content) started as a result of fungus growth. It became possible to distinguish between the spectra from infected and healthy samples as shown in Figure 13 and Figure 14. Also, the difference became more apparent as the growth of the fungus increased as shown in Figure 15 and Figure 16. These results are in agreement with previous studies (Gamon & Surfus, 1999; Mahlein *et al.*, 2010; Sankaran *et al.*, 2011).

Furthermore, when internal changes in the affected fruit occur before external changes (before symptoms appear), the acquired spectra are different (Sasaki *et al.*, 1998; Wu *et al.*, 2008). This is what was observed when comparing the spectra of affected samples from zero-day to the fourth day of injection, where the difference was clear between the spectra as shown in Figure 17. To remove slope variation, MSC was carried out to the same spectra as shown in Figure 18. These results are in arrangement with several previous studies (Shen *et al.*, 2019; Yuan *et al.*, 2014).

First derivatives (1st D) with Savitzky-Golay (SG) were carried out to reduce drift and noise in acquired spectra from infected samples as shown in Figure 19.

Tomato contains a high percentage of water approximately 90-95% (Rizk, 2018). The highest absorbing waves (*i.e.* bands at 819, 945, 969, 972, 989 nm) were in the NIR region as a result of vibration in the O-H bond (Liu, 2016). Also, the result of these absorption bands due to the high content of carbohydrates (C-H bond) and proteins (N-H bond) (*i.e.* bands at 1013 and 1087 nm) (Chen *et al.*, 2008; Lopez *et al.*, 2017). While in the VIS region the highest absorption bands (560, 580 and 606 nm) were due to pigments *i.e.* chlorophylls and carotenoids. The weak absorption bands associated with the small content of carbohydrates and proteins that were consumed by the fungus. These results

are in agreement with previous studies (Abu-Khalaf, 2015; Flores *et al.*, 2009; Shen *et al.*, 2019; Xu *et al.*, 2009).

The spectra can be affected by the external factors, as well as the properties of fruits such as the water content and others as mentioned previously. Moreover, as the number of samples increases, it becomes difficult to distinguish if they are infected or intact through the spectra only. Therefore, MVDA *e.g.* PCA, is needed to extract useful information from the acquired spectra.

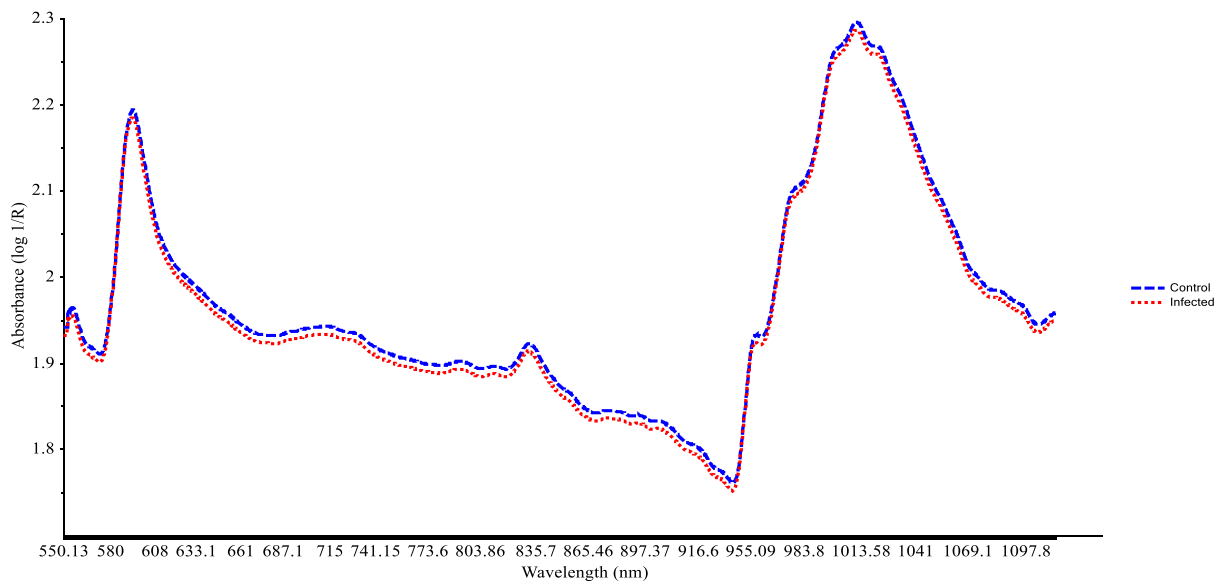


Figure 12. A representative spectral curve of VIS/NIR (550-1100 nm) in zero-day of inoculation. Control sample (blue) and infected sample (red), with Savitzky-Golay (SG) smoothing preprocessing effect.

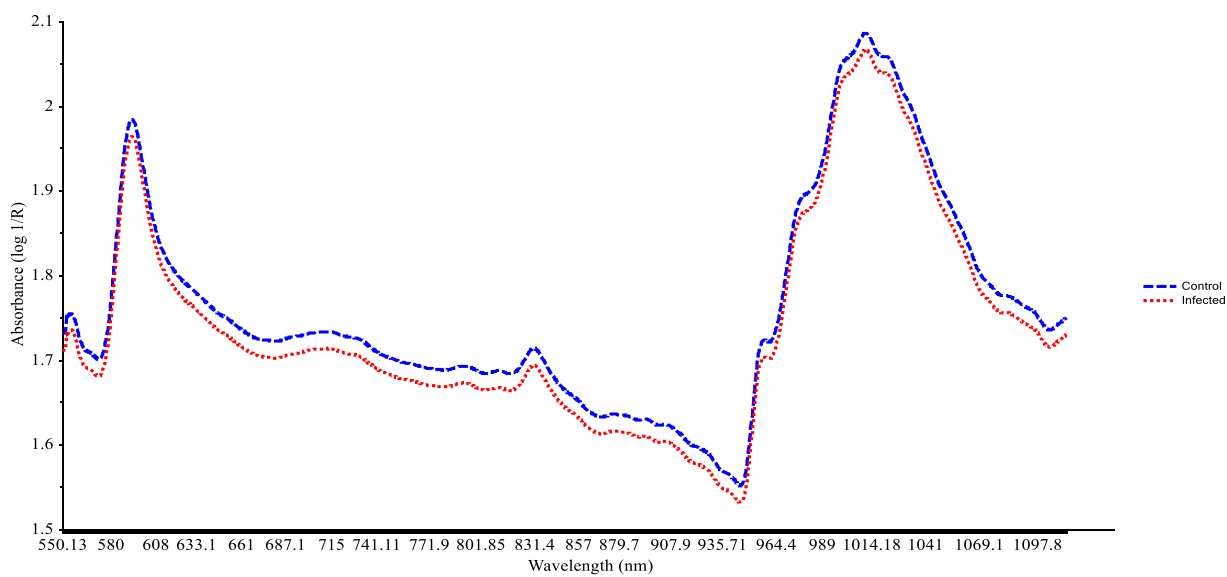


Figure 13. A representative spectral curve of VIS/NIR (550-1100 nm) in the first day of inoculation. Control sample (blue) and infected sample (red), with Savitzky-Golay (SG) smoothing preprocessing effect.

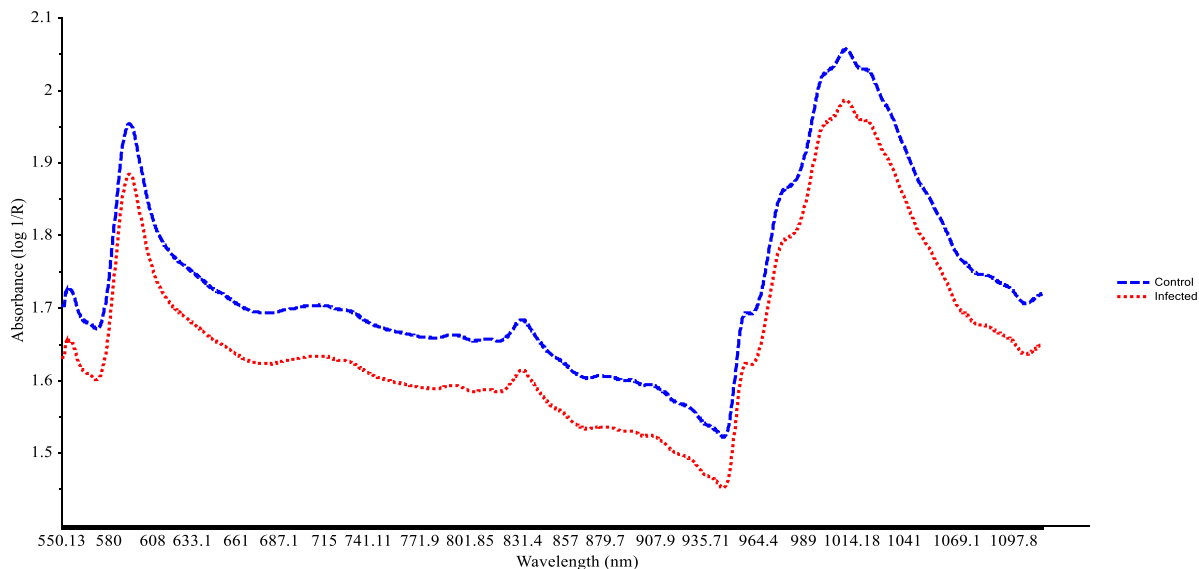


Figure 14. A representative spectral curve of VIS/NIR (550-1100 nm) in the second day of inoculation. Control sample (blue) and infected sample (red), with Savitzky-Golay (SG) smoothing preprocessing effect.

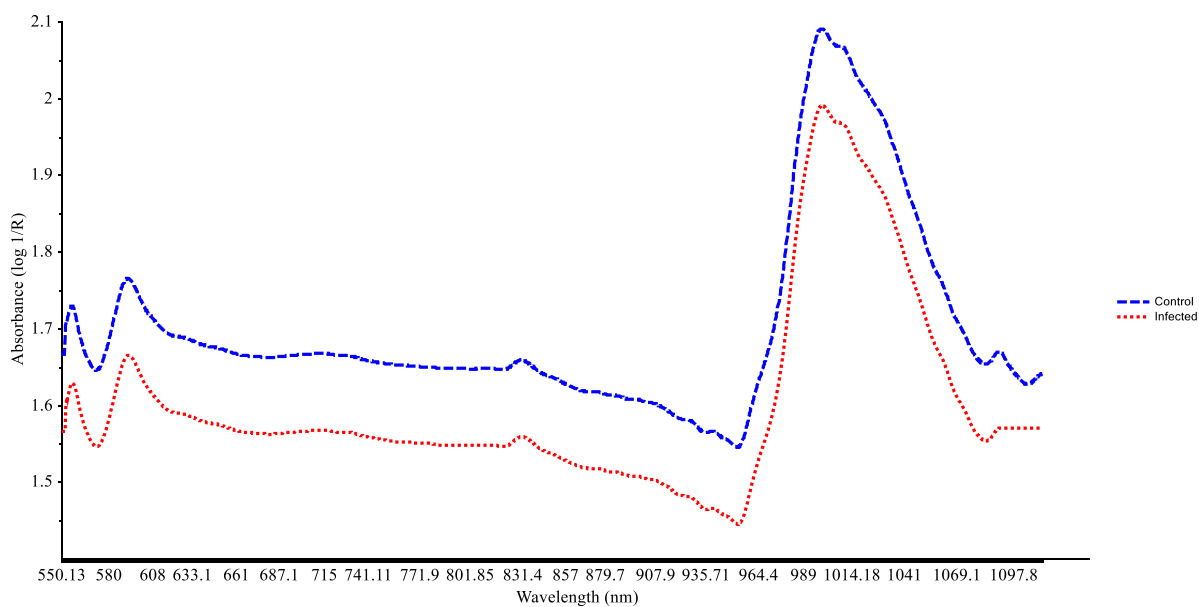


Figure 15. A representative spectral curve of VIS/NIR (550-1100 nm) in the third day of inoculation. Control sample (blue) and infected sample (red), with Savitzky-Golay (SG) smoothing preprocessing effect.

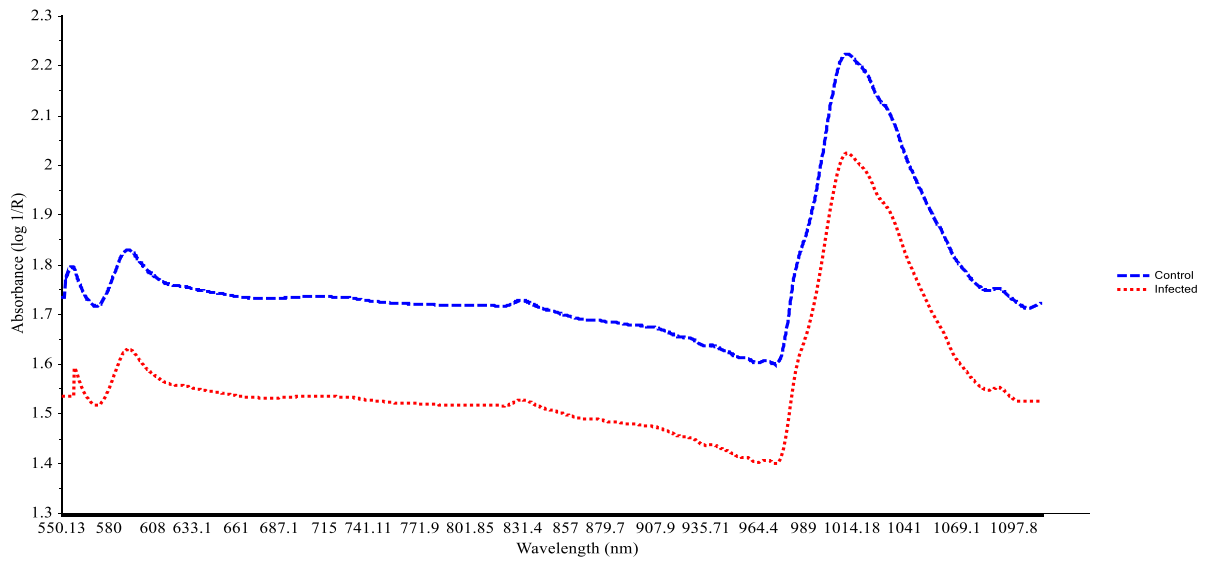


Figure 16. A representative spectral curve of VIS/NIR (550-1100 nm) in the fourth day of inoculation. Control sample (blue) and infected sample (red), with Savitzky-Golay (SG) smoothing preprocessing effect.

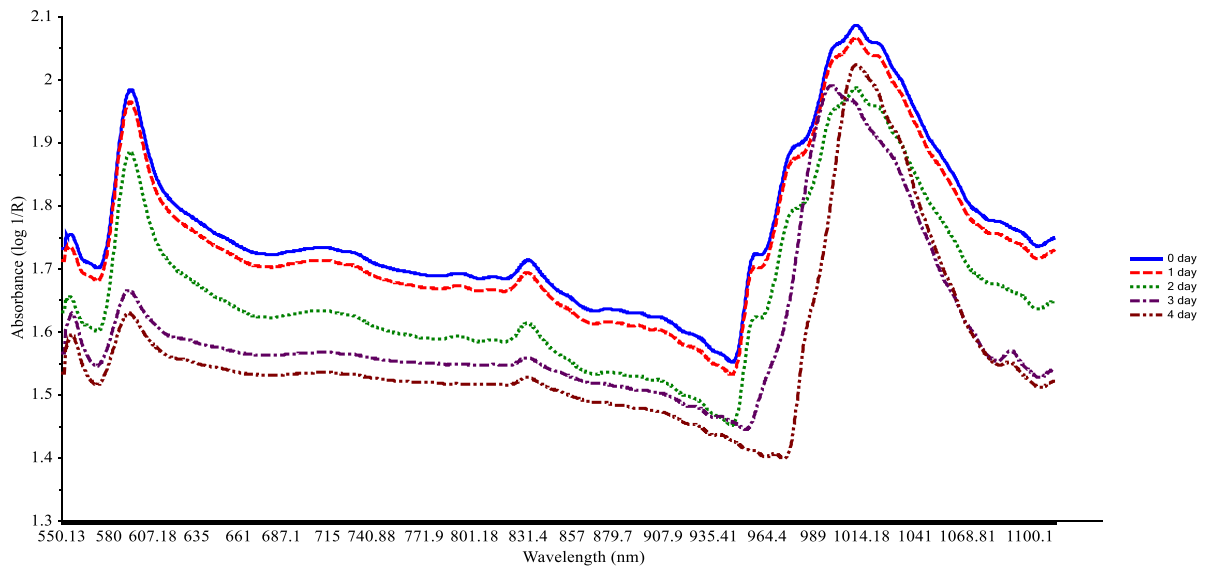


Figure 17. A representative typical VIS/NIR (550-1100 nm) spectral curve of infected samples for all days of inoculation. Zero-day (blue), the first day (red), the second day (green), the third day (purple) and the fourth day (brown), with Savitzky-Golay (SG) smoothing preprocess.

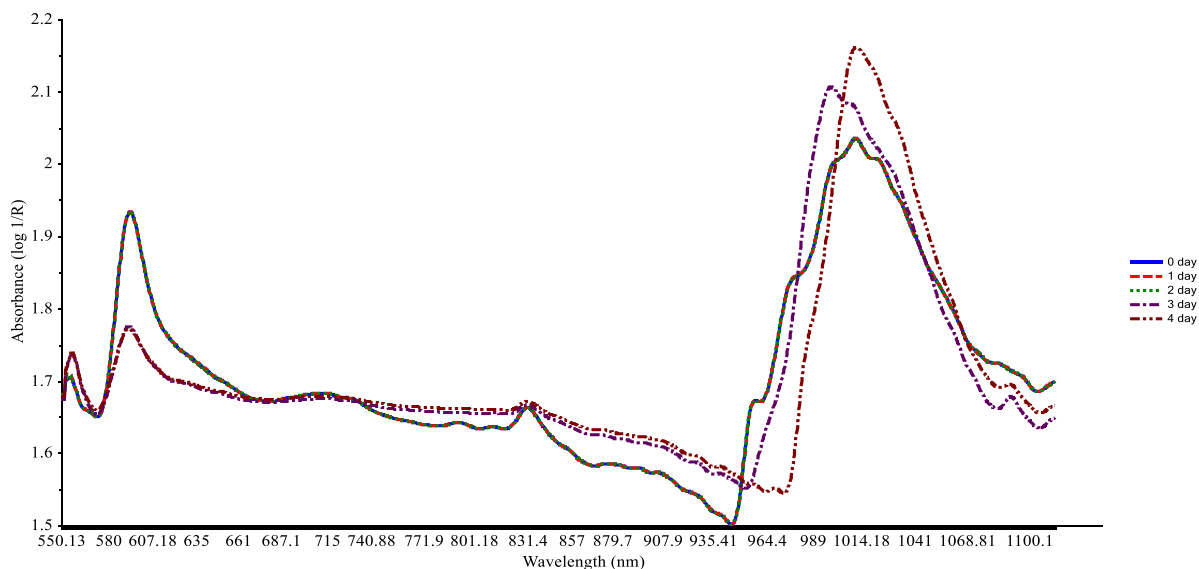


Figure 18. The effect of multiplicative scatter correction (MSC) preprocessing on the spectra of infected samples for all days of inoculation. Zero-day (blue), the first day (red), the second day (green), the third day (purple) and the fourth day (brown).

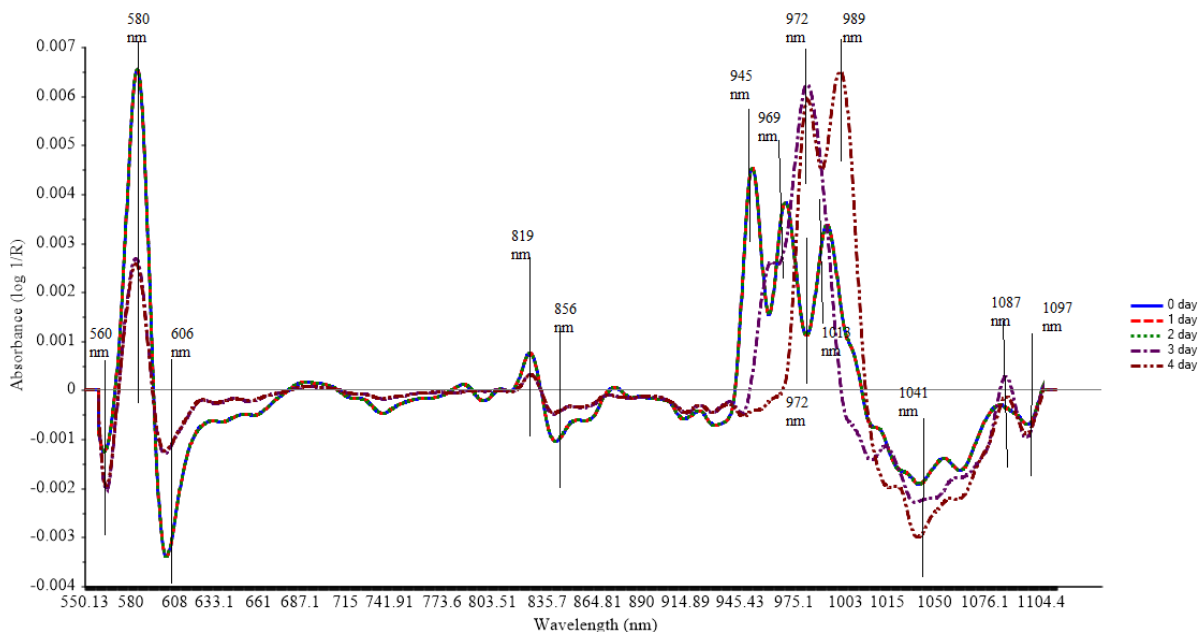


Figure 19. The effect of first derivatives (1st D) with Savitzky-Golay (SG) preprocessing on the spectra of infected samples. Zero-day (blue), the first day (red), the second day (green), the third day (purple) and the fourth day (brown).

4.3 PCA

Principal component analysis (PCA) was carried out for the VIS/NIR region (550-1100 nm) of the zero-day, first day, second day, third day and fourth day of inoculation the fungi.

In zero-day, two principal components (PCs) for VIS/NIR region explained 81% of the total variance. In this PCA, the results showed no distinguishing between control and infected samples as shown in Figure 20. In the first day, two PCs for VIS/NIR region explained 74% of the total variance. Where the results showed the ability of VIS/NIR spectroscopy to distinguish between infected and control, but the two groups (*i.e.* infected and control group) are still close to each other, as shown in Figure 21. In the second, the third and the fourth day the two PCs for VIS/NIR region explained about 99% of the total variance as shown in Figure 22 to Figure 24.

Our PCA results showed the possibility for VIS/NIR spectroscopy to distinguish between healthy and unhealthy samples after 24 hours (*i.e.* one day) of inoculation. While the visual symptoms began to appear in the third and fourth days of injection. Also, the PCA models for the second, third and fourth day showed that the control samples were completely separated from infected samples, where it was observed that the distance began to increase between the two groups (*i.e.* control and infected group).

In addition, the PCA of all day (*i.e.* zero-day, the first day, second day, third day and fourth day of inoculation) was carried out after calculating the average for the infected samples (*i.e.* 60 infected samples for each day were divided on 3 (number of varieties)). Where two PCs for VIS/NIR region explained 98% of the total variance as shown in Figure 25. The results showed the ability of the PCA to separate between zero-day and the first day with some overlap, but there is a complete separation between the second, third and fourth day of the injection. Also, the distance between zero-day and the first day increased from the second day. Moreover, the distance becomes more increase between the second and third days of infection. All the PCA results are in agreement with previous studies (Bagheri & Mohamadi-Monavar, 2020; Marin-Ortiz *et al.*, 2020; Mogollon *et al.*, 2019; Moscetti *et al.*, 2015; Sankaran *et al.*, 2011).

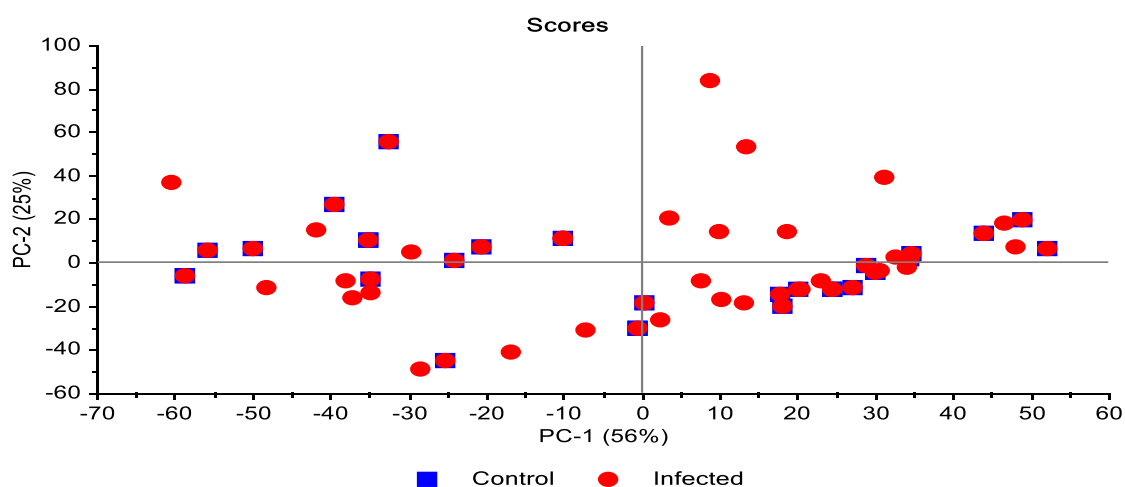


Figure 20. Scores plot of PCA model based on VIS/NIR (550-1100 nm) spectra for zero-day. Control (blue) and infected (red). Two PCs explained 81% of the total variance.

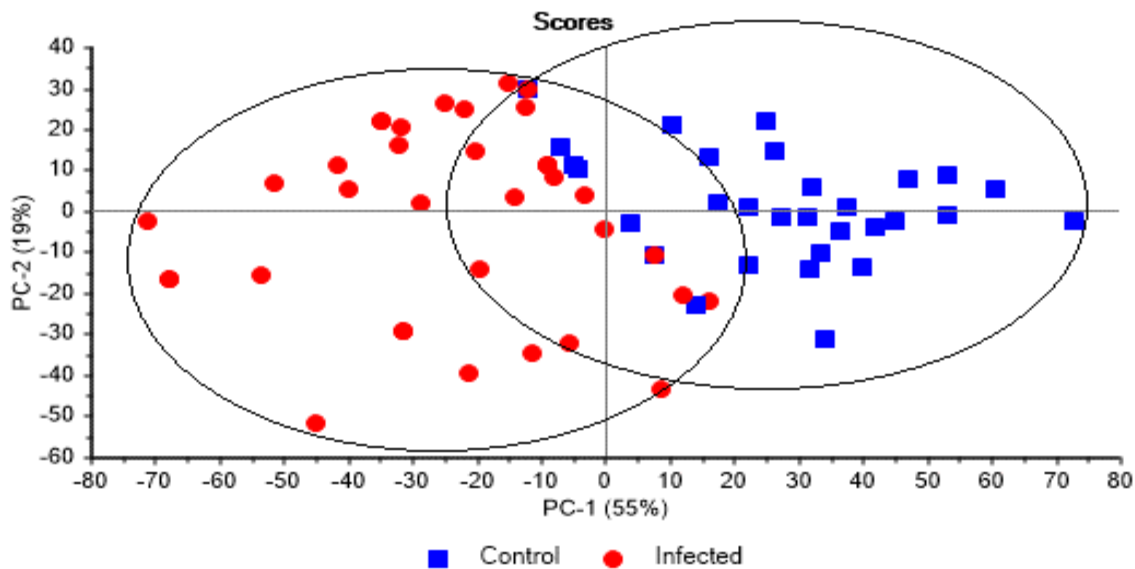


Figure 21. Scores plot of PCA model based on VIS/NIR (550-1100 nm) spectra for the first day. Control (blue) and infected (red). Two PCs explained 74% of the total variance.

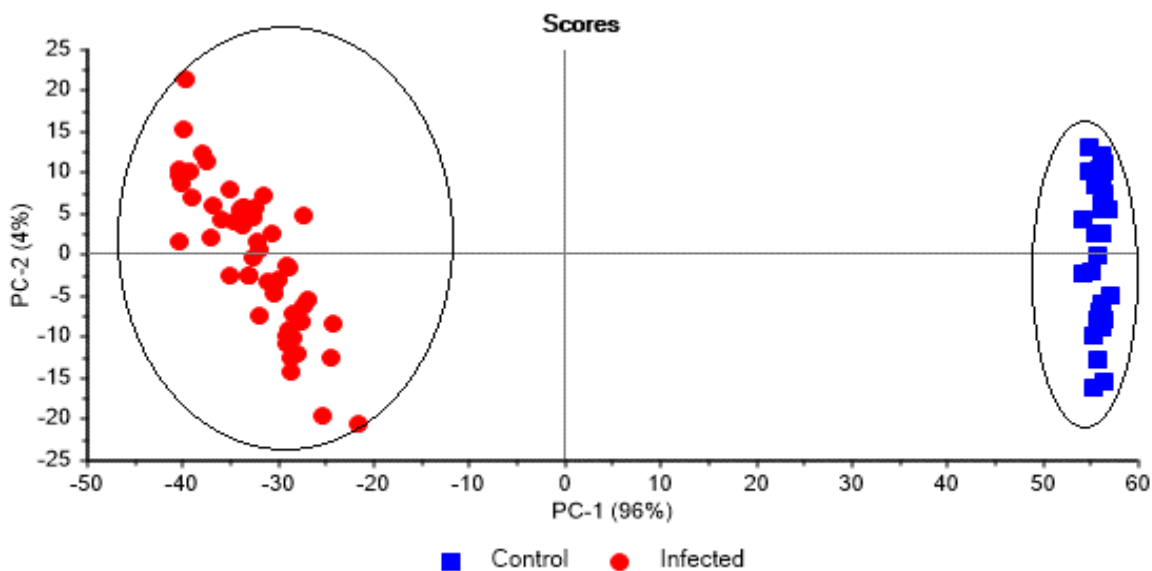


Figure 22. Scores plot of the PCA model based on VIS/NIR (550-1100 nm) spectra for the second day. Control (blue) and infected (red). Two PCs explained 100% of the total variance.

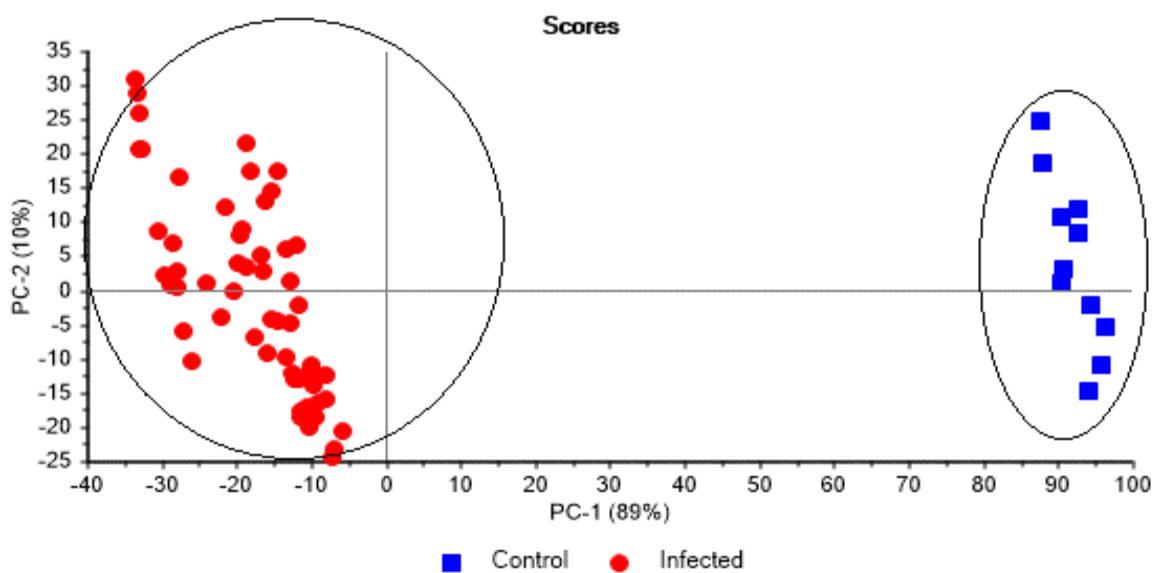


Figure 23. Scores plot of the PCA model based on VIS/NIR (550-1100 nm) spectra for the third day. Control (blue) and infected (red). Two PCs explained 99% of the total variance.

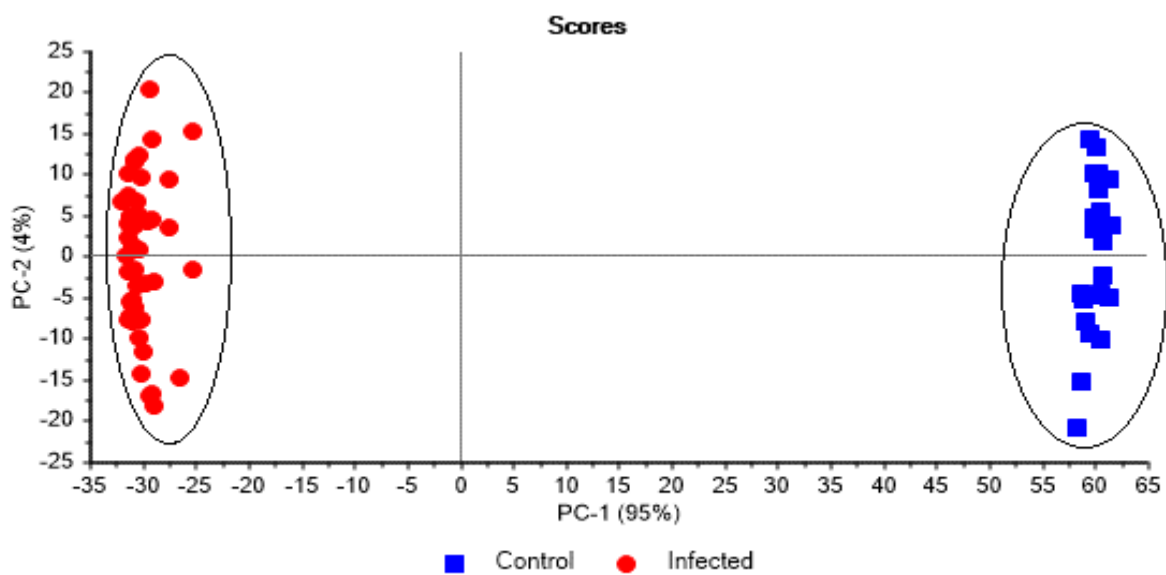


Figure 24. Scores plot of the PCA model based on VIS/NIR (550-1100 nm) spectra for the fourth day. Control (blue) and infected (red). Two PCs explained 99% of the total variance.

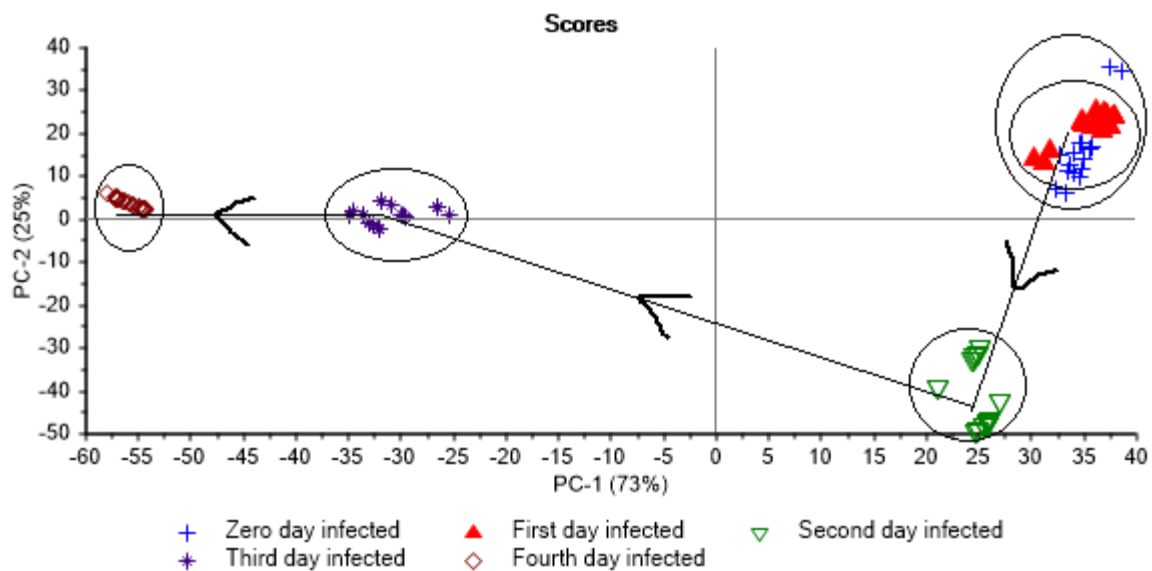


Figure 25. Scores plot of the PCA model based on VIS/NIR (550-1100 nm) spectra for the average of infected samples for all days. Zero-day infected (blue), the first day infected (red), the second day infected (green), the third day infected (purple) and the fourth day infected (brown). Two PCs explained 98% of the total variance.

4.3.1 Prediction test

The prediction test of the PCA models was carried out for the first day of the VIS/NIR region (550-1100 nm), as shown in Figure 26, where the VIS/NIR spectroscopy was able successfully to predict the new sample based on the PCA model for the VIS/NIR region at this stage.

Prediction test was also performed for the second and third day (Figure 27 and Figure 28), where the results showed the ability of the model to distinguish successfully between the new infected and healthy samples.

Finally, the prediction of the PCA model was applied to the VIS/NIR region for the fourth day, as shown in Figure 29, and the results showed its ability to distinguish between the new samples. The prediction test was carried out in much previous research to examine the ability of the PCA model to predict any new sample (Bair *et al.*, 2006; Ghasemi *et al.*, 2019).

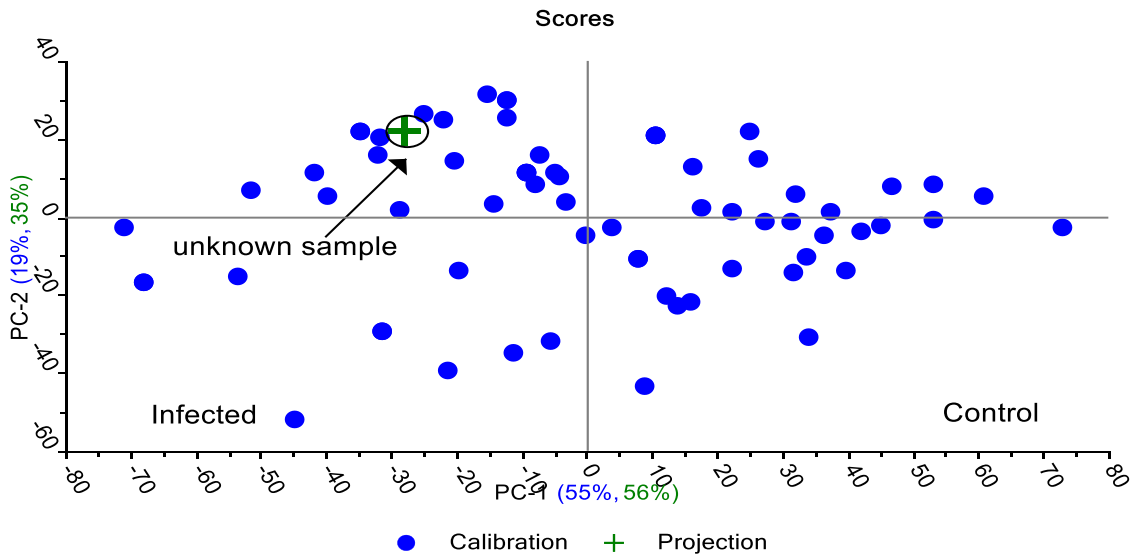


Figure 26. Prediction test for unknown sample based on the PCA model for the first day for VIS/NIR (550-1100 nm). Two PCs for calibration set explained 74% of the total variance and two PCs for projection set explained 91% of the total variance.

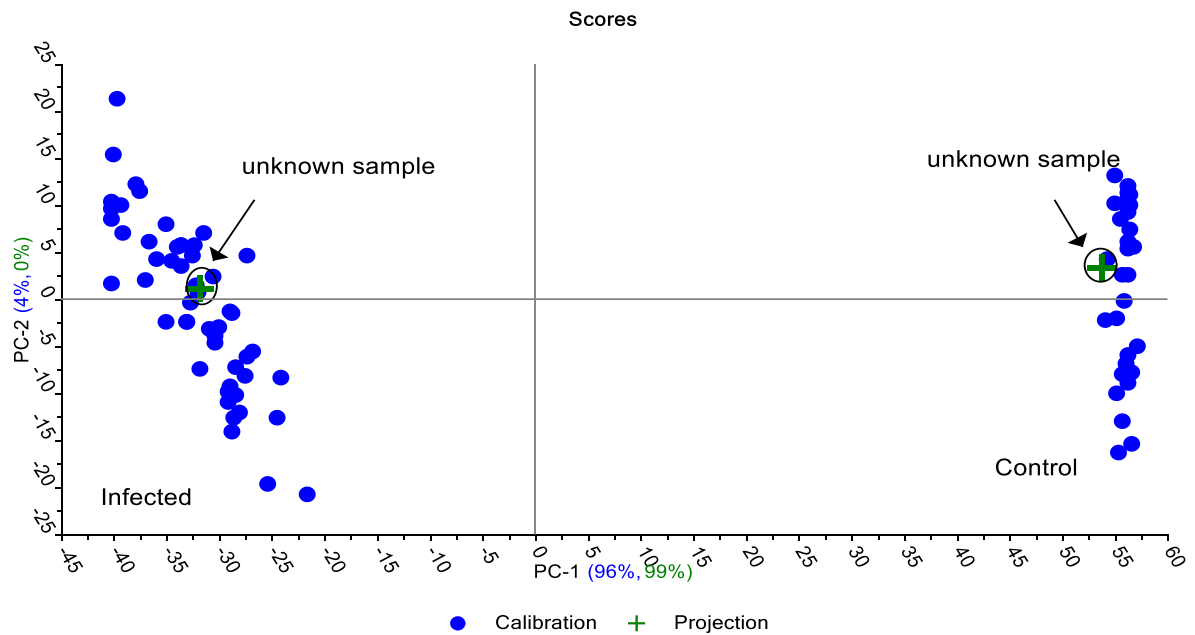


Figure 27. Prediction test for unknown samples based on the PCA model for the second day for VIS/NIR (550-1100 nm). Two PCs for calibration set explained 100% of the total variance and one PC for projection set explained 99% of the total variance.

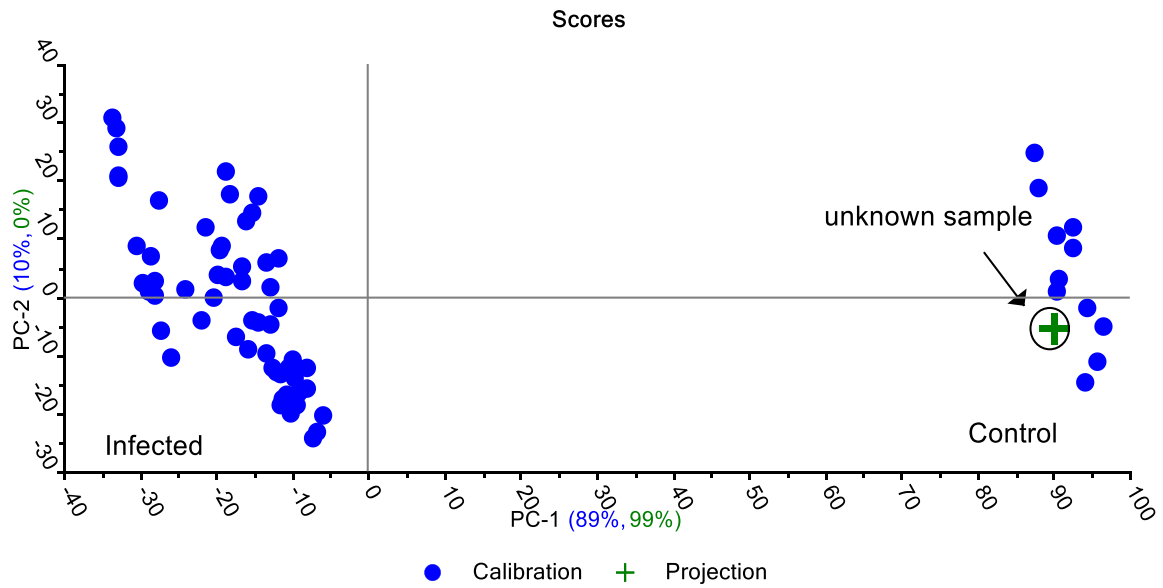


Figure 28. Prediction test for an unknown sample based on the PCA model for the third day for VIS/NIR (550-1100 nm). Two PCs for calibration set explained 99% of the total variance and one PC for projection set explained 99% of the total variance.

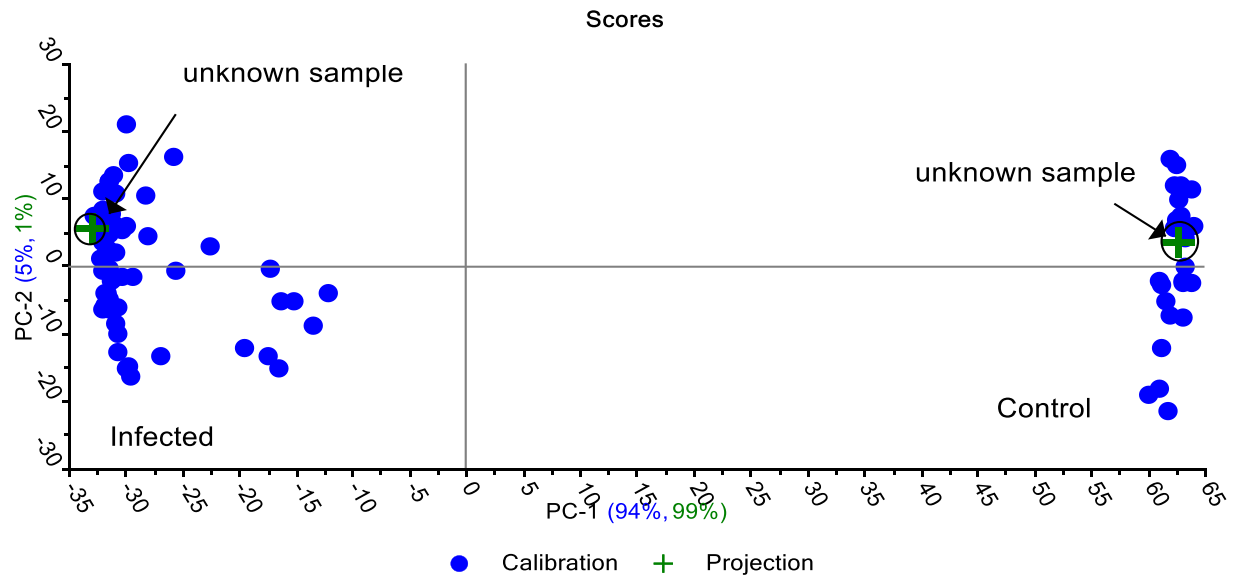


Figure 29. Prediction test for unknown samples based on the PCA model for the fourth day for VIS/NIR (550-1100 nm). Two PCs for calibration set explained 99% of the total variance and two PCs for projection set explained 100% of the total variance.

4.4 Resistant variety to gray mold according to time decay

The results showed that all varieties of tomato used in the study (Harver, Izmer and Ekram) are sensitive to gray mold disease, as shown in Figure 30, where symptoms appeared on these varieties with the same period approximately and the same degree of infection. As previously discussed, the tomato crop is sensitive to gray mold disease (Dean *et al.*, 2012; Smith *et al.*, 2014; Williamson *et al.*, 2007).

However, there are no local studies to prove the resistance of these varieties to gray mold disease, especially in the post-harvest chain.

Based on the information available from the Ministry of Agriculture, gray mold disease was recorded as the most common disease affecting tomato fruits, and there is no resistant variety available for it among these used varieties.

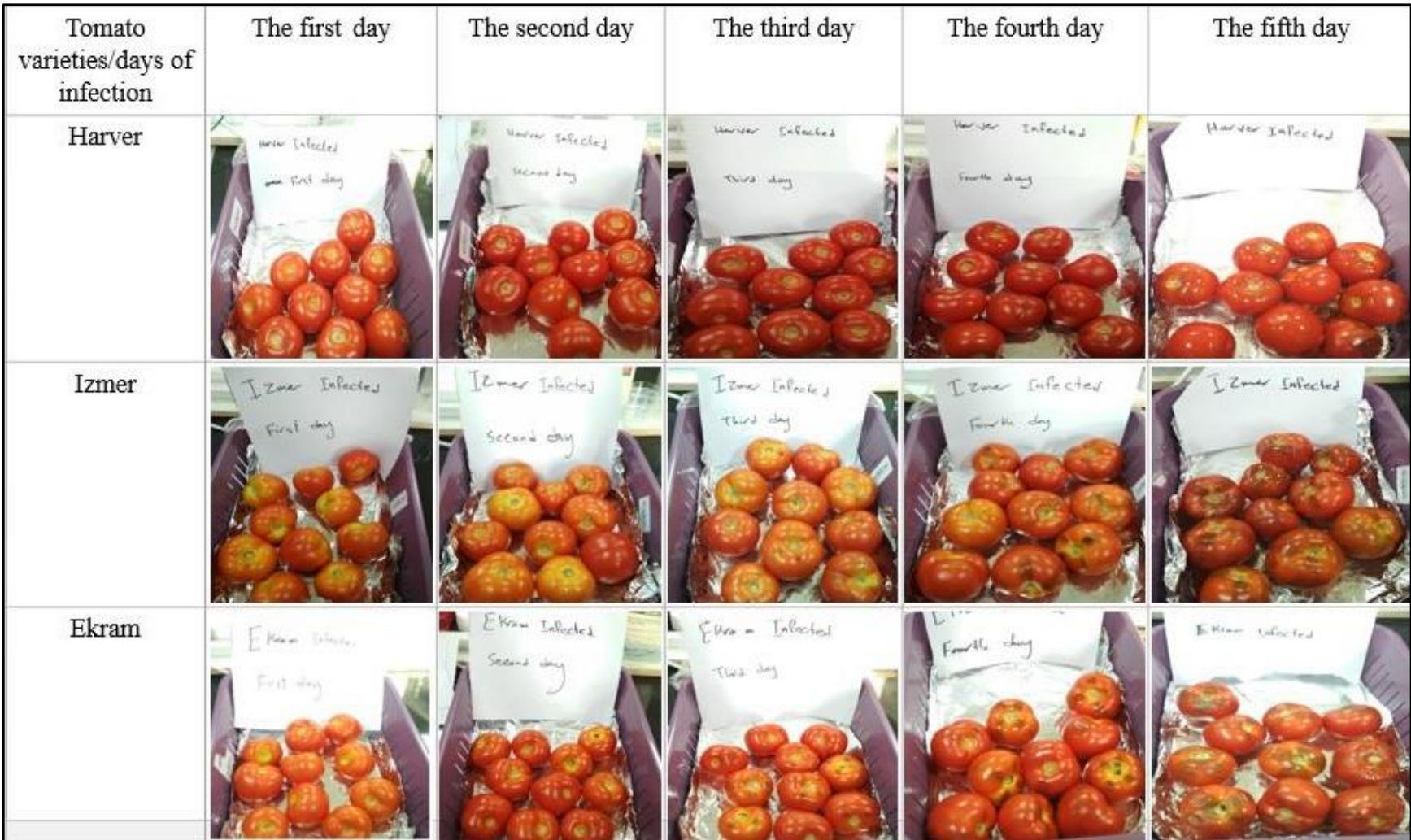


Figure 30. Illustration to compare the appearance of gray mold disease symptoms on tomato varieties to determine which ones are resistant and which are sensitive during storage days.

5 Conclusion and recommendation

In conclusion, specific primers, *i.e.* C729+/C729-, BC108+/BC653- and BNTF1/BNTR1, could identify *B. cinerea* fungus using PCR technique. Also, the results of the study showed that there is no variety resistant to gray mold disease that affects tomato fruits among the three varieties used in this study.

The non-destructive VIS/NIR technique was able to sense the *B. cinerea* fungus in early-stage on tomato fruits. Moreover, VIS/NIR spectroscopy could predict a new sample, as well as could classify the healthy and unhealthy sample.

In addition, the results open a wide door for using a portable VIS/NIR spectroscopy in agricultural industries (on-line and in-line) to ensure that fruits are free from diseases. And it suggests the probability of using this study for development on-line optical system that can be applied directly in the field for the early detection of infected plants.

For future studies, diversity in plant diseases, as well as diversity in plant varieties, is required to build more models using VIS/NIR spectroscopy combined MVDA techniques for early detection of plant disease. Furthermore, work to find a tomato variety resistant to gray mold disease is needed to reduce the economic losses.

6 Abstract in Arabic (الملخص بالعربي)

استشعار وجود الفطر المسبب للعفن الرمادي في البندورة باستخدام الاشعة المرئية

والقريبة من تحت الحمراء

الطالبة: خديجة محمد خميس نجار

المشرف: الدكتور نواف أبو خلف

الملخص

يعتبر محصول البندورة من المحاصيل المهمة عالميا. كما يتعرض هذا المحصول الى العديد من الامراض خاصة الفطرية التي تسبب خسائر اقتصادية هائلة، حيث يعتبر مرض العفن الرمادي الذي يسببه فطر *Botrytis cinerea* من اشهر الامراض التي تصيب ثمار البندورة خاصة ما بعد الحصاد. تم تصنيف هذا الفطر من بين اكثر عشرة فطريات تصيب النباتات وتسبب خسائر اقتصادية، فهو يقع بالمرتبة الثانية بعد فطر *Magnaporthe oryzae* الذي يصيب محصول الارز.

الكشف المبكر عن المرض قبل ظهور الاعراض يعتبر من احد الاسباب التي يمكن ان توفر 50% من الخسائر على مستوى الحقل وكذلك على مستوى الصناعات الزراعية. على مرور السنين، تم استخدام طرق عديدة للكشف عن الممرضات التي تصيب النباتات منها ما كان بالعين المجردة ومنها مخبريا مثل الاعتماد على المجهر الضوئي. ولكن هذه الطرق تعتبر مستهلكة للوقت، مدمرة وتحتاج لظهور الاعراض بداية. لذا كان التوجه نحو استخدام تقنيات غير مدمرة مثل تقنية التحليل بالاشعة المرئية والقريبة من تحت الحمراء (VIS/NIR spectroscopy) للكشف عن الامراض النباتية.

تم تطبيق هذه التقنية ذات الموجة القصيرة (400-1300 نانوميتر) والمتوسطة (400-2500 نانوميتر) في دراسات سابقة للكشف عن امراض عديدة تصيب النباتات. تتميز هذه التقنية بانها سريعة، غير مدمرة ولا تحتاج الى تحضير

مسبق للعينات. لكن من ناحية اخرى، مازال هناك بعض المحددات لاستخدامها مثل الحاجة الى خبرة لتحليل النتائج وبناء النماذج الرياضية. ولكن يمكن تجاوز هذه المحددات باستخدام الطرق الحديثة في تحليل النتائج.

على حد علمنا، لم يتم تطبيق تقنية (VIS/NIR) بطول موجة 1100-550 نانوميتر للكشف عن مرض العفن الرمادي على ثمار البندورة. لذلك، كان الهدف من هذه الدراسة استخدام تقنية الاشعة المرئية والقريبة من تحت الحمراء VIS/NIR لاستشعار وجود العفن الرمادي في المراحل الاولى على ثمار البندورة.

بداية تم عزل فطر *B. cinerea* من عينات بندورة مصابة وتعريفه باستخدام تقنية polymerase chain reaction (PCR). بعد ذلك، تم جمع 90 عينة بندورة من ثلاث اصناف مختلفة (هارفر، اكرام وازمير) اختيرت هذه العينات خالية من الامراض وبتوصية من مديرية زراعة طولكرم. تم حقن 20 عينة من كل صنف بالمرض و10 عينات تركت كمرجع. تم فحص جميع العينات باستخدام جهاز الطيف المرئي والاشعة القريبة من تحت الحمراء بطول موجة 1100-550 نانوميتر والموجود بمختبرات مركز خضوري للبحوث الزراعي-جامعة فلسطين التقنية-خضوري بشكل يومي ابتداء من اليوم الاول للحقن الى اليوم الخامس للحقن، ثم جمعت القراءات لتحلل لاحقا.

بعد استخدام برنامج لتحليل البيانات متغير المتعددات (النمذجة الرياضية) (MDVA) عن طريق تحليل المكون الرئيسي principle component analysis (PCA). اظهرت النتائج قدرة تقنية الطيف المرئي و الاشعة القريبة من تحت الحمراء على التمييز بين العينات المصابة والسليمة في المراحل الاولى للمرض. حيث كان المكون الرئيسي (principle component PC) لليوم الثاني مفسرا ما نسبته 100% من التغير الكلي لمنطقة الطيف المرئي والاشعة القريبة من تحت الحمراء (1100-550 نانوميتر) معا. وايضا لليوم الثالث والرابع للحقن، كانت نتائج PC تقريبا مفسرة ما نسبته 99% من التغير الكلي. كما استطاع التمييز بين العينات المصابة لليوم الثاني والثالث والرابع للحقن عن بعضها البعض بينما كان هناك تداخل بين اليوم صفر واليوم الاول للحقن حيث كانت نتائج PC مفسرة ما نسبته 98% من التغير الكلي. وكذلك عن مراقبة الاصناف الثلاثة لتحديد اي منها مقاوم للمرض، وجد ان جميع هذه الاصناف حساسة لمرض العفن الرمادي حيث ظهرت عليها الاعراض بنفس الوقت ونفس الدرجة تقريبا.

اهم الاستنتاجات والتوصيات التي تم التوصل اليها من خلال هذه الدراسة، حسب نتائج PCR فانه يمكن استخدام احدى هذه البرايمرات (primers) لتعريف فطر *B. cinerea* (C729+/C729-, BC108+/BC563- and BNTF1/BNTR1). كذلك حسب نتائج PCA فانه يمكن استخدام تقنية الطيف المرئي والاشعة القريبة من تحت الحمراء بطول موجة 550-1100 نانوميتر للكشف المبكر عن مرض العفن الرمادي. وهذا يفتح المجال امام استخدام الجهاز المتنقل (portable VIS/NIR spectroscopy) في الصناعات الزراعية وكذلك يمكن تطبيقه مباشرة في الحقل. للدراسات المستقبلية، هناك حاجة الى التنوع في اصناف النباتات كذلك، التنوع بامراض النباتات للتاكيد على قدرة تقنية VIS/NIR مع استخدام تقنية MDVA في الكشف المبكر عن الامراض. بالاضافة الى العمل على ايجاد صنف بندورة مقاوم لمرض العفن الرمادي للتقليل من الخسائر الاقتصادية.

References

- Abu-Khalaf, N. & Salman, M. (2013). Detecting plant diseases using visible/near infrared spectroscopy. *NIR news*, 24, 12-25.
- Abu-Khalaf, N. (2015). Sensing tomato's pathogen using Visible/Near infrared (VIS/NIR) spectroscopy and multivariate data analysis (MVDA). *Palestine Technical University Research Journal*, 3, 12-22.
- Abu-Khalaf, N. & Bennedsen, B. S. (2004). Near infrared (NIR) technology and multivariate data analysis for sensing taste attributes of apples. *International Agrophysics*, 18, 203-212.
- Abu-Khalaf, N., Bennedsen, B. S., & Bjorn, G. K. (2004). Distinguishing carrots characteristics by near infrared (NIR) reflectance and multivariate data analysis. *Agricultural Engineering International: CIGR Journal, Manuscript FP 03 012*.
- Alander, J. T., Bochko, V., Martinkauppi, B., Saranwong, S., & Mantere, T. (2013). A review of optical nondestructive visual and near-infrared methods for food quality and safety. *International Journal of Spectroscopy*, 2013.
- Ali, M. M., Bachik, N. A., Muhadi, N. A., Yusof, T. N. T., & Gomes, C. (2019). Non-Destructive Techniques of Detecting Plant Diseases: A Review. *Physiological and Molecular Plant Pathology*, 108, 101426-101470.
- Amigo, J. M., Marti, I., & Gowen, A. (2013). Hyperspectral imaging and chemometrics: a perfect combination for the analysis of food structure, composition and quality. In *Data handling in science and technology* (28 ed., pp. 343-370). Elsevier.

- Angioni, A., Porcu, L., & Dedola, F. (2012). Determination of famoxadone, fenamidone, fenhexamid and iprodione residues in greenhouse tomatoes. *Pest Management Science*, 68, 543-547.
- Arah, I. K., Amaglo, H., Kumah, E. K., & Ofori, H. (2015). Preharvest and postharvest factors affecting the quality and shelf life of harvested tomatoes: a mini review. *International Journal of Agronomy*, 2015.
- ARIJ (2015). *Palestinian Agricultural Production and Marketing between Reality and Challenges*. Bethlehem - Palestine: ARIJ.
- Bagheri, N. & Mohamadi-Monavar, H. (2020). Early Detection of Fire Blight Disease of Pome Fruit Trees Using Visible-NIR Spectrometry and Dimensionality Reduction Methods. *Journal of Agricultural Machinery*, 10, 37-48.
- Bahri, A., Nawar, S., Selmi, H., Amraoui, M., Rouissi, H., & Mouazen, A. M. (2019). Application of visible and near-infrared spectroscopy for evaluation of ewes milk with different feeds. *Animal Production Science*, 59, 1190-1200.
- Bair, E., Hastie, T., Paul, D., & Tibshirani, R. (2006). Prediction by supervised principal components. *Journal of the American Statistical Association*, 101, 119-137.
- Baranowski, P., Mazurek, W., Wozniak, J., & Majewska, U. (2012). Detection of early bruises in apples using hyperspectral data and thermal imaging. *Journal of Food Engineering*, 110, 345-355.

- Barnes, R. J., Dhanoa, M. S., & Lister, S. J. (1989). Standard normal variate transformation and de-trending of near-infrared diffuse reflectance spectra. *Applied Spectroscopy*, *43*, 772-777.
- Beghi, R., Buratti, S., Giovenzana, V., Benedetti, S., & Guidetti, R. (2017). Electronic nose and visible-near infrared spectroscopy in fruit and vegetable monitoring. *Reviews in Analytical Chemistry*, *36*, 2191-2215.
- Beghi, R., Giovenzana, V., Tugnolo, A., & Guidetti, R. (2018). Application of visible/near infrared spectroscopy to quality control of fresh fruits and vegetables in large-scale mass distribution channels: a preliminary test on carrots and tomatoes. *Journal of the Science of Food and Agriculture*, *98*, 2729-2734.
- Biancolillo, A. & Marini, F. (2018). Chemometric methods for spectroscopy-based pharmaceutical analysis. *Frontiers in Chemistry*, *6*, 576-605.
- Bienkowski, D., Aitkenhead, M. J., Lees, A. K., Gallagher, C., & Neilson, R. (2019). Detection and differentiation between potato (*Solanum tuberosum*) diseases using calibration models trained with non-imaging spectrometry data. *Computers and Electronics in Agriculture*, *167*, 105056-105068.
- Borges, A. V., Saraiva, R. M., & Maffia, L. A. (2014). Key factors to inoculate *Botrytis cinerea* in tomato plants. *Summa Phytopathologica*, *40*, 221-225.
- Brereton, R. G., Jansen, J., Lopes, J., Marini, F., Pomerantsev, A., Rodionova, O. et al. (2017). Chemometrics in analytical chemistry—part I: history, experimental design and data analysis tools. *Analytical and Bioanalytical Chemistry*, *409*, 5891-5899.

- Bustin, S. A. (2017). How to speed up the polymerase chain reaction. *Biomolecular Detection and Quantification*, 12, 10-14.
- Butz, P., Hofmann, C., & Tauscher, B. (2005). Recent developments in noninvasive techniques for fresh fruit and vegetable internal quality analysis. *Journal of Food Science*, 70, R131-R141.
- Carlos, M. O. J., Nathalia, G. T., Veronica, B. F., & Maria, H. C. L. (2019). Linking physiological parameters with visible/near-infrared leaf reflectance in the incubation period of vascular wilt disease. *Saudi Journal of Biological Sciences*, 27, 88-99.
- Cattaneo, T. M. & Stellari, A. (2019). NIR Spectroscopy as a Suitable Tool for the Investigation of the Horticultural Field. *Agronomy*, 9, 503-521.
- Cen, H., He, Y., & Huang, M. (2007). Combination and comparison of multivariate analysis for the identification of orange varieties using visible and near infrared reflectance spectroscopy. *European Food Research and Technology*, 225, 699-705.
- Chen, J. Y., Miao, Y., Sato, S., & Zhang, H. (2008). Near infrared spectroscopy for determination of the protein composition of rice flour. *Food Science and Technology Research*, 14, 132-138.
- Cortes, V., Blasco, J., Aleixos, N., Cubero, S., & Talens, P. (2019a). Monitoring strategies for quality control of agricultural products using visible and near-infrared spectroscopy: A review. *Trends in Food Science & Technology*, 85, 138-148.

- Cortes, V., Cubero, S., Blasco, J., Aleixos, N., & Talens, P. (2019b). In-line Application of Visible and Near-Infrared Diffuse Reflectance Spectroscopy to Identify Apple Varieties. *Food and Bioprocess Technology*, *12*, 1021-1030.
- Cremonez, V. G., Klitzke, R. J., Silva, E. J. d., Muniz, G. I. B. d., & Nisgoski, S. (2019). Influence of Age on the Discrimination of *Tectona grandis* by VIS/NIR Spectroscopy. *Floresta e Ambiente*, *26*, 2179-2187.
- Dean, R., van Kan, J. A., Pretorius, Z. A., Hammond-Kosack, K. E., Di Pietro, A., Spanu, P. D. et al. (2012). The Top 10 fungal pathogens in molecular plant pathology. *Molecular Plant Pathology*, *13*, 414-430.
- Dickens, J. E. (2010). Overview of process analysis and PAT. *Process Analytical Technology*, 1-15.
- Dos Santos, C. A. T., Lopo, M., Pascoa, R. N., & Lopes, J. A. (2013). A review on the applications of portable near-infrared spectrometers in the agro-food industry. *Applied Spectroscopy*, *67*, 1215-1233.
- Droby, S. & Lichter, A. (2007). Post-harvest Botrytis infection: etiology, development and management. In *Botrytis: Biology, pathology and control* (pp. 349-367). Dordrecht: Springer.
- El-Mesery, H. S., Mao, H., & Abomohra, A. E.-F. (2019). Applications of Non-destructive Technologies for Agricultural and Food Products Quality Inspection. *Sensors*, *19*, 846-869.

- Elad, Y. & Shtienberg, D. (1995). Botrytis cinerea in greenhouse vegetables: chemical, cultural, physiological and biological controls and their integration. *Integrated Pest Management Reviews*, 1, 15-29.
- Elad, Y., Williamson, B., Tudzynski, P., & Delen, N. (2007). Botrytis spp. and diseases they cause in agricultural systems—an introduction. In *Botrytis: Biology, pathology and control* (pp. 1-8). Dordrecht: Springer.
- Fahrentrapp, J., Michl, G., & Breuer, M. (2013). Quantitative PCR assay for detection of bois noir phytoplasmas in grape and insect tissue. *Vitis*, 52, 85-89.
- Fahrentrapp, J., Ria, F., Geilhausen, M., & Panassiti, B. (2019). Detection of gray mold leaf infections prior to visual symptom appearance using a five-band multispectral sensor. *Frontiers in Plant Science*, 10, 628-642.
- Fan, X., Zhang, J., Yang, L., Wu, M., Chen, W., & Li, G. (2015). Development of PCR-based assays for detecting and differentiating three species of Botrytis infecting broad bean. *Plant Disease*, 99, 691-698.
- FAO (2018). *Post-harvest management of tomato for quality and safety assurance*. Rome, Italy: FAO.
- FAO (2019). Statistical database of the FAO. faostat [Electronic version]. Available: <http://faostat.fao.org/site/339/default.aspx>. Access date: 2/1/2020

- Farber, C., Mahnke, M., Sanchez, L., & Kurouski, D. (2019). Advanced Spectroscopic Techniques for Plant Disease Diagnostics. A Review. *Trends in Analytical Chemistry*, *118*, 43-49.
- Farres, S., Srata, L., Fethi, F., & Kadaoui, A. (2019). Argan oil authentication using visible/near infrared spectroscopy combined to chemometrics tools. *Vibrational Spectroscopy*, *102*, 79-84.
- Feng, L., Zhang, M., Adhikari, B., & Guo, Z. (2019). Nondestructive Detection of Postharvest Quality of Cherry Tomatoes Using a Portable NIR Spectrometer and Chemometric Algorithms. *Food Analytical Methods*, *12*, 914-925.
- Feng, Y. Z. & Sun, D. W. (2013). Determination of total viable count (TVC) in chicken breast fillets by near-infrared hyperspectral imaging and spectroscopic transforms. *Talanta*, *105*, 244-249.
- Fillinger, S. & Elad, Y. (2016). *Botrytis: the fungus, the pathogen and its management in agricultural systems*. Springer.
- Flores, K., Sanchez, M. T., Perez-Marin, D., Guerrero, J. E., & Garrido-Varo, A. (2009). Feasibility in NIRS instruments for predicting internal quality in intact tomato. *Journal of Food Engineering*, *91*, 311-318.
- Gamon, J. A. & Surfus, J. S. (1999). Assessing leaf pigment content and activity with a reflectometer. *The New Phytologist*, *143*, 105-117.

- Gao, P., Qin, J., Li, D., & Zhou, S. (2018). Inhibitory effect and possible mechanism of a *Pseudomonas* strain QBA5 against gray mold on tomato leaves and fruits caused by *Botrytis cinerea*. *Plos One*, *13*, e0190932-e0190947.
- Garcia-Sanchez, F., Galvez-Sola, L., Martinez-Nicolas, J. J., Muelas-Domingo, R., & Nieves, M. (2017). Using near-infrared spectroscopy in agricultural systems. *Developments in Near-Infrared Spectroscopy*, *2017*, 97-130.
- Geladi, P., MacDougall, D., & Martens, H. (1985). Linearization and scatter-correction for near-infrared reflectance spectra of meat. *Applied Spectroscopy*, *39*, 491-500.
- Ghasemi, P., Aslani, M., Rollins, D. K., & Williams, R. C. (2019). Principal component analysis-based predictive modeling and optimization of permanent deformation in asphalt pavement: elimination of correlated inputs and extrapolation in modeling. *Structural and Multidisciplinary Optimization*, *59*, 1335-1353.
- Gindro, K., Pezet, R., Viret, O., & Richter, H. (2005). Development of a rapid and highly sensitive direct-PCR assay to detect a single conidium of *Botrytis cinerea* Pers.: Fr in vitro and quiescent forms in planta. *Vitis-Geilweilerhof*, *44*, 139-143.
- Gowen, A. A., O'Donnell, C. P., Cullen, P. J., Downey, G., & Frias, J. M. (2007). Hyperspectral imaging—an emerging process analytical tool for food quality and safety control. *Trends in Food Science & Technology*, *18*, 590-598.
- Goyette, B., Charles, M. T., Vigneault, C., & Raghavan, V. (2010). Effect of hyperbaric treatment on quality attributes of tomato fruits. In (pp. 1-13). American Society of Agricultural and Biological Engineers.

- Guifang, W., Hai, M., & Xin, P. (2015). Identification of varieties of natural textile fiber based on Vis/NIR spectroscopy technology. *2015 IEEE Advanced Information Technology, Electronic and Automation Control Conference (IAEAC)*, 585-589.
- Hahn, F. (2009). Actual pathogen detection: sensors and algorithms-A review. *Algorithms*, 2, 301-338.
- Hair, J. F., Black, W. C., Babin, B. J., Anderson, R. E., & Tatham, R. L. (1998). *Multivariate data analysis*. (5 ed.) (vols. 3) Prentice hall Upper Saddle River, NJ.
- Harmon, C. L. (2013). *Plant disease diagnosis in the age of PCR: Improving the toolbox and increasing credibility*. University of Florida.
- He, Y., Zhang, Y., Pereira, A. G., Gomez, A. H., & Wang, J. (2005). Nondestructive determination of tomato fruit quality characteristics using VIS/NIR spectroscopy technique. *International Journal of Information Technology*, 11, 97-108.
- Hennebert, G. L. (1973). Botrytis and Botrytis-like genera. *Persoonia*, 7, 183-204.
- Hua, L., Yong, C., Zhanquan, Z., Boqiang, L., Guozheng, Q., & Shiping, T. (2018). Pathogenic mechanisms and control strategies of Botrytis cinerea causing post-harvest decay in fruits and vegetables. *Food Quality and Safety*, 2, 111-119.
- Huang, H., Yu, H., Xu, H., & Ying, Y. (2008). Near infrared spectroscopy for on/in-line monitoring of quality in foods and beverages: A review. *Journal of Food Engineering*, 87, 303-313.

- Huang, Y., Lu, R., & Chen, K. (2018). Assessment of tomato soluble solids content and pH by spatially-resolved and conventional Vis/NIR spectroscopy. *Journal of Food Engineering*, 236, 19-28.
- Isaksson, T. & Naes, T. (1988). The effect of multiplicative scatter correction (MSC) and linearity improvement in NIR spectroscopy. *Applied Spectroscopy*, 42, 1273-1284.
- Kandpal, L. M. & Cho, B. K. (2014). A review of the applications of spectroscopy for the detection of microbial contaminations and defects in agro foods. *Journal of Biosystems Engineering*, 39, 215-226.
- Karstang, T. V. & Manne, R. (1992). Optimized scaling: a novel approach to linear calibration with closed data sets. *Chemometrics and Intelligent Laboratory Systems*, 14, 165-173.
- Kawamura, K., Tsujimoto, Y., Rabenarivo, M., Asai, H., Andriamananjara, A., & Rakotoson, T. (2017). Vis-NIR spectroscopy and PLS regression with waveband selection for estimating the total C and N of paddy soils in Madagascar. *Remote Sensing*, 9, 1081-1094.
- Khaled, A. Y., Abd Aziz, S., Bejo, S. K., Nawi, N. M., Seman, I. A., & Onwude, D. I. (2018). Early detection of diseases in plant tissue using spectroscopy—applications and limitations. *Applied Spectroscopy Reviews*, 53, 36-64.
- Kumar, R. & Sharma, V. (2017). A novel combined approach of diffuse reflectance UV-Vis-NIR spectroscopy and multivariate analysis for non-destructive examination of

blue ballpoint pen inks in forensic application. *Spectrochimica Acta Part A: Molecular and Biomolecular Spectroscopy*, 175, 67-75.

- Kumaravelu, C. & Gopal, A. (2015). A review on the applications of Near-Infrared spectrometer and Chemometrics for the agro-food processing industries. In (pp. 8-12). IEEE.
- Lee, K. M., Herrman, T. J., Nansen, C., & Yun, U. (2013). Application of Raman spectroscopy for qualitative and quantitative detection of fumonisins in ground maize samples. *International Journal of Regulatory Science*, 1, 1-14.
- Leyronas, C., Duffaud, M., & Nicot, P. C. (2012). Compared efficiency of the isolation methods for *Botrytis cinerea*. *Mycology*, 3, 221-225.
- Li, Y., Wang, H., Zhang, Y., & Martin, C. (2018). Can the world's favorite fruit, tomato, provide an effective biosynthetic chassis for high-value metabolites? *Plant Cell Reports*, 37, 1443-1450.
- Liu, S., Hai, F., & Jiang, J. (2017). Sensitivity to fludioxonil of *Botrytis cinerea* isolates from tomato in Henan Province of China and characterizations of fludioxonil-resistant mutants. *Journal of Phytopathology*, 165, 98-104.
- Liu, Y., Sun, X., Zhou, J., Zhang, H., & Yang, C. (2010). Linear and nonlinear multivariate regressions for determination sugar content of intact Gannan navel orange by VIS–NIR diffuse reflectance spectroscopy. *Mathematical and Computer Modelling*, 51, 1438-1443.

- Liu, Y. (2016). *Non-destructive Phenotyping of Postharvest Quality Traits of Tomatoes and Strawberries*. (pp. 1-49). Netherlands.
- Lopez, M. G., Garcia-Gonzalez, A. S., & Franco-Robles, E. (2017). Carbohydrate analysis by NIRS-Chemometrics. *Developments in Near-Infrared Spectroscopy*, 10, 67208-67224.
- Luypaert, J., Massart, D. L., & Vander Heyden, Y. (2007). Near-infrared spectroscopy applications in pharmaceutical analysis. *Talanta*, 72, 865-883.
- Mahlein, A. K., Steiner, U., Dehne, H. W., & Oerke, E. C. (2010). Spectral signatures of sugar beet leaves for the detection and differentiation of diseases. *Precision Agriculture*, 11, 413-431.
- Marin-Ortiz, J. C., Gutierrez-Toro, N., Botero-Fernandez, V., & Hoyos-Carvajal, L. M. (2020). Linking physiological parameters with visible/near-infrared leaf reflectance in the incubation period of vascular wilt disease. *Saudi Journal of Biological Sciences*, 27, 88-99.
- Marti, R., Rosello, S., & Cebolla-Cornejo, J. (2016). Tomato as a source of carotenoids and polyphenols targeted to cancer prevention. *Cancers*, 8, 58-86.
- Martinelli, F., Scalenghe, R., Davino, S., Panno, S., Scuderi, G., Ruisi, P. et al. (2015). Advanced methods of plant disease detection. A review. *Agronomy for Sustainable Development*, 35, 1-25.

- Mirmajlessi, S. M., Destefanis, M., Gottsberger, R. A., M+ñnd, M., & Loit, E. (2015). PCR-based specific techniques used for detecting the most important pathogens on strawberry: a systematic review. *Systematic Reviews*, 4, 9-40.
- Mogollon, M. R., Jara, A. F., Contreras, C., & Zoffoli, J. P. (2019). Quantitative and qualitative VIS-NIR models for early determination of internal browning in 'Cripps Pink' apples during cold storage. *Postharvest Biology and Technology*, 161, 111060-111071.
- Mohammadi, S., Aroiee, H., Aminifard, M. H., & Jahanbakhsh, V. (2012). In vitro and in vivo antifungal activities of the essential oils of various plants against strawberry grey mould disease agent *Botrytis cinerea*. *Archives of Phytopathology and Plant Protection*, 45, 2474-2484.
- Morawski, R. Z. & Mi-Okina, A. (2016). Application of principal components analysis and signal-to-noise ratio for calibration of spectrophotometric analysers of food. *Measurement*, 79, 302-310.
- Moscetti, R., Haff, R. P., Stella, E., Contini, M., Monarca, D., Cecchini, M. et al. (2015). Feasibility of NIR spectroscopy to detect olive fruit infested by *Bactrocera oleae*. *Postharvest Biology and Technology*, 99, 58-62.
- Narayanasamy, P. (2010). *Microbial Plant Pathogens-Detection and Disease Diagnosis::: Viral and Viroid Pathogens*. (3 ed.) Springer Science & Business Media.
- Nasir, M. U., Hussain, S., & Jabbar, S. (2015). Tomato processing, lycopene and health benefits: A review. *Science Letters*, 3, 1-5.

- Ncama, K., Magwaza, L. S., Mditshwa, A., & Tesfay, S. Z. (2018). Application of Visible to Near-Infrared Spectroscopy for Non-Destructive Assessment of Quality Parameters of Fruit. In *Infrared Spectroscopy-Principles, Advances, and Applications* (IntechOpen).
- Nicolai, B. M., Beullens, K., Bobelyn, E., Peirs, A., Saeys, W., Theron, K. I. et al. (2007). Nondestructive measurement of fruit and vegetable quality by means of NIR spectroscopy: A review. *Postharvest Biology and Technology*, *46*, 99-118.
- Nicolai, B. M., Defraeye, T., De Ketelaere, B., Herremans, E., Hertog, M. L., Saeys, W. et al. (2014). Nondestructive measurement of fruit and vegetable quality. *Annual Review of Food Science and Technology*, *5*, 285-312.
- Pande, S., Singh, G., Rao, J. N., Bakr, M. A., Chaurasia, P. C. P., Joshi, S. et al. (2001). Integrated management of botrytis gray mold of chickpea. *India: International Crops Research Institute for the Semi-Arid Tropics*, *61*, 32-66.
- Pasquini, C. (2018). Near infrared spectroscopy: A mature analytical technique with new perspectives—A review. *Analytica Chimica Acta*, *1026*, 8-36.
- Peirs, A., Scheerlinck, N., & Nicolai, B. M. (2003). Temperature compensation for near infrared reflectance measurement of apple fruit soluble solids contents. *Postharvest Biology and Technology*, *30*, 233-248.
- Petrasch, S., Silva, C. J., Mesquida-Pesci, S. D., Gallegos, K., van den Abeele, C., Papin, V. et al. (2019). Infection strategies deployed by *Botrytis cinerea*, *Fusarium*

- acuminatum, and *Rhizopus stolonifer* as a function of tomato fruit ripening stage. *Frontiers in Plant Science*, *10*, 223-240.
- Porep, J. U., Kammerer, D. R., & Carle, R. (2015). On-line application of near infrared (NIR) spectroscopy in food production. *Trends in Food Science & Technology*, *46*, 211-230.
- Qin, J. & Lu, R. (2008). Measurement of the optical properties of fruits and vegetables using spatially resolved hyperspectral diffuse reflectance imaging technique. *Postharvest Biology and Technology*, *49*, 355-365.
- Qu, J. H., Liu, D., Cheng, J. H., Sun, D. W., Ma, J., Pu, H. et al. (2015). Applications of near-infrared spectroscopy in food safety evaluation and control: A review of recent research advances. *Critical Reviews in Food Science and Nutrition*, *55*, 1939-1954.
- Quinet, M., Angosto, T., Yuste-Lisbona, F. J., Blanchard-Gros, R., Bigot, S., Martinez, J. P. et al. (2019). Tomato Fruit Development and Metabolism. *Frontiers in Plant Science*, *10*, 1554-1607.
- Rady, A., Sugiharto, S., & Adedeji, A. A. (2018). Evaluation of carrot quality using visible-near infrared spectroscopy and multivariate analysis. *Journal of Food Research*, *7*, 80-93.
- Rigotti, S., Gindro, K., Richter, H., & Viret, O. (2002). Characterization of molecular markers for specific and sensitive detection of *Botrytis cinerea* Pers.: Fr. in strawberry (*Fragaria* ananassa* Duch.) using PCR. *FEMS Microbiology Letters*, *209*, 169-174.

- Rigotti, S., Viret, O., & Gindro, K. (2006). Two new primers highly specific for the detection of *Botrytis cinerea* Pers. Fr. *Phytopathologia Mediterranea*, 45, 253-260.
- Rizk, H. (2018). Automated early plant disease detection and grading system: Development and implementation. (pp.1-163). Cairo.
- Sadilek, T. (2019). Perception of Food Quality by Consumers: Literature Review. *European Research Studies*, 22, 57-67.
- Saeyns, W., Do Trong, N. N., Van Beers, R., & Nicolai, B. M. (2019). Multivariate calibration of spectroscopic sensors for postharvest quality evaluation: A review. *Postharvest Biology and Technology*, 158, 110981-111000.
- Sankaran, S., Ehsani, R., Inch, S. A., & Ploetz, R. C. (2012). Evaluation of visible-near infrared reflectance spectra of avocado leaves as a non-destructive sensing tool for detection of laurel wilt. *Plant Disease*, 96, 1683-1689.
- Sankaran, S., Mishra, A., Maja, J. M., & Ehsani, R. (2011). Visible-near infrared spectroscopy for detection of Huanglongbing in citrus orchards. *Computers and Electronics in Agriculture*, 77, 127-134.
- Sannakki, S. S., Rajpurohit, V. S., Nargund, V. B., Kumar, A., & Yallur, P. S. (2011). Leaf disease grading by machine vision and fuzzy logic. *International Journal of Computer Technology and Applications*, 2, 1709-1716.
- Sasaki, Y., Okamoto, T., Imou, K., & Torii, T. (1998). Automatic diagnosis of plant disease-Spectral reflectance of healthy and diseased leaves. *IFAC Proceedings Volumes*, 31, 145-150.

- Savitzky, A. & Golay, M. J. (1964). Smoothing and differentiation of data by simplified least squares procedures. *Analytical Chemistry*, *36*, 1627-1639.
- Schaare, P. N. & Fraser, D. G. (2000). Comparison of reflectance, interactance and transmission modes of visible-near infrared spectroscopy for measuring internal properties of kiwifruit (*Actinidia chinensis*). *Postharvest Biology and Technology*, *20*, 175-184.
- Scholthof, K.-B. G., Adkins, S., Czosnek, H., Palukaitis, P., Jacquot, E., Hohn, T. et al. (2011). Top 10 plant viruses in molecular plant pathology. *Molecular Plant Pathology*, *12*, 938-954.
- Sharma, G. P. R. R. & Pandey, R. R. (2010). Influence of culture media on growth, colony character and sporulation of fungi isolated from decaying vegetable wastes. *Journal of Yeast and Fungal Research*, *1*, 157-164.
- Sharon Ruth, K., Uma Makeswari, T., & Leo Pauline, S. (2018). NIR Spectroscopy to Detect Nutrients and Disease in Plants. *International Journal of Pure and Applied Mathematics*, *119*, 733-740.
- Shen, F., Zhao, T., Jiang, X., Liu, X., Fang, Y., Liu, Q. et al. (2019). On-line detection of toxigenic fungal infection in wheat by visible/near infrared spectroscopy. *Food Science and Technology*, *109*, 216-224.
- Shi, J. F. & Sun, C. Q. (2017). Isolation, identification, and biocontrol of antagonistic bacterium against *Botrytis cinerea* after tomato harvest. *Brazilian Journal of Microbiology*, *48*, 706-714.

- Shirane, N., Masuko, M., & Hayashi, Y. (1988). Nuclear behavior and division in germinating conidia of *Botrytis cinerea*. *Phytopathology (USA)*, *78*, 1627-1630.
- Skolik, P., Morais, C. L., Martin, F. L., & McAinsh, M. R. (2019). Determination of developmental and ripening stages of whole tomato fruit using portable infrared spectroscopy and Chemometrics. *BMC Plant Biology*, *19*, 236-280.
- Smith, J. E., Mengesha, B., Tang, H., Mengiste, T., & Bluhm, B. H. (2014). Resistance to *Botrytis cinerea* in *Solanum lycopersicoides* involves widespread transcriptional reprogramming. *BMC Genomics*, *15*, 334-352.
- Song, J. Y., Lim, J. H., Nam, M. H., Kim, H. G., & Kim, B. S. (2008). Development of PCR Primers for Specific Identification and Detection of *Botrytis cinerea* on Tomato. *The Korean Journal of Mycology*, *36*, 138-143.
- Soylu, E. M., Kurt, S., & Soyly, S. (2010). In vitro and in vivo antifungal activities of the essential oils of various plants against tomato grey mould disease agent *Botrytis cinerea*. *International Journal of Food Microbiology*, *143*, 183-189.
- Steinier, J., Termonia, Y., & Deltour, J. (1972). Smoothing and differentiation of data by simplified least square procedure. *Analytical Chemistry*, *44*, 1906-1909.
- Sun, D. W. (2010). *Hyperspectral imaging for food quality analysis and control*. (1 ed.) UK: Elsevier.
- Takam, G. H. F., Tatsinkou, F. B., Mbah, J. A., Bate, P. N. N., & Ngemenya, M. N. (2019). Morphological and PCR characterisation of fungi isolated from tomato postharvest,

- and potential control of fruit spoilage by antifungal plant extracts. *International Food Research Journal*, 26, 123-131.
- Teye, E., Huang, X. y., & Afoakwa, N. (2013). Review on the potential use of near infrared spectroscopy (NIRS) for the measurement of chemical residues in food. *American Journal Food Science Technology*, 1, 1-8.
- Viskelis, P., Radzevicius, A., Urbonaviciene, D., Viskelis, J., Karkleliene, R., & Bobinas, C. (2015). Biochemical parameters in tomato fruits from different cultivars as functional foods for agricultural, industrial, and pharmaceutical uses. *Plants for The Future*, 10, 60873.
- Wang, H., Peng, J., Xie, C., Bao, Y., & He, Y. (2015). Fruit quality evaluation using spectroscopy technology: a review. *Sensors*, 15, 11889-11927.
- Wei, Y., Xu, M., Wu, H., Tu, S., Pan, L., & Tu, K. (2016). Defense response of cherry tomato at different maturity stages to combined treatment of hot air and *Cryptococcus laurentii*. *Postharvest Biology and Technology*, 117, 177-186.
- Weiberg, A., Wang, M., Lin, F. M., Zhao, H., Zhang, Z., Kaloshian, I. et al. (2013). Fungal small RNAs suppress plant immunity by hijacking host RNA interference pathways. *Science*, 342, 118-123.
- Williamson, B., Tudzynski, B., Tudzynski, P., & van Kan, J. A. (2007). Botrytis cinerea: the cause of grey mould disease. *Molecular Plant Pathology*, 8, 561-580.
- Wilson, A. D. (2013). Diverse applications of electronic-nose technologies in agriculture and forestry. *Sensors*, 13, 2295-2348.

- Wold, S., Esbensen, K., & Geladi, P. (1987). Principal component analysis, *Chemometr. Intell. Lab.*, 2, 37–52.
- Wu, D., Feng, L., Zhang, C., & He, Y. (2008). Early detection of *Botrytis cinerea* on eggplant leaves based on visible and near-infrared spectroscopy. *Transactions of the ASABE*, 51, 1133-1139.
- Xu, H. r., Yu, P., Fu, X. p., & Ying, Y. b. (2009). On-site variety discrimination of tomato plant using visible-near infrared reflectance spectroscopy. *Journal of Zhejiang University Science B*, 10, 126-132.
- You, J., Guo, J., Yuan, Q., Guo, X., Gao, L., Duan, Y. et al. (2019). *Botrytis cinerea* causing grey mould on *Epimedium brevicornum* Maxim in China. *Canadian Journal of Plant Pathology*, 1-7.
- Yuan, L., Huang, Y., Loraamm, R. W., Nie, C., Wang, J., & Zhang, J. (2014). Spectral analysis of winter wheat leaves for detection and differentiation of diseases and insects. *Field Crops Research*, 156, 199-207.
- Zaid, A., Abu-Khalaf, N., Mudalal, S., & Petracci, M. (2020). Differentiation between normal and white striped turkey breasts by visible/near infrared spectroscopy and multivariate data analysis. *Food Science of Animal Resources*, 40, 96-105.
- Zhang, C., Feng, X., Wang, J., Liu, F., He, Y., & Zhou, W. (2017). Mid-infrared spectroscopy combined with chemometrics to detect *Sclerotinia* stem rot on oilseed rape (*Brassica napus* L.) leaves. *Plant Methods*, 13, 39-48.

Zhang, J., Huang, Y., Pu, R., Gonzalez-Moreno, P., Yuan, L., Wu, K. et al. (2019).

Monitoring plant diseases and pests through remote sensing technology: A review.

Computers and Electronics in Agriculture, 165, 104943-104957.

Zhang, Z., Qin, G., Li, B., & Tian, S. (2014). Infection assays of tomato and apple fruit by the fungal pathogen *Botrytis cinerea*. *Bio-Protocol*, 4, 1-5.

Zude, M. (2008). *Optical monitoring of fresh and processed agricultural crops*. CRC press.

The End